Approaching the metal-insulator transition

T. R. Kirkpatrick
Institute for Physical Science and Technology, and Department of Physics and Astronomy, University of Maryland, College Park, Maryland 20742

D. Belitz*
Department of Physics and Materials Science Institute, University of Oregon, Eugene, Oregon 97403 and Center for Superconductivity Research, University of Maryland, College Park, Maryland 20742
(Received 13 October 1989)

The problem of disordered interacting electrons is considered. We study a model for a generic disordered Fermi liquid without cooper pairs and in the absence of any spin-flip mechanisms. We prove to within logarithmic accuracy that there is a stable renormalization-group fixed point to all orders in a loop expansion. We prove that the conductivity exponent at this fixed point is identically equal to zero, while the spin-diffusion constant scales to zero with an exponent $\gamma=4+O(d-2)$. By an explicit two-loop calculation we then show that this fixed point is suppressed by logarithmic terms, but a sizeable scaling region persists. The main conclusion is that the metal-insulator transition is preceded on the metallic side by a near instability in the spin system. There is a scaling region leading from a spin-diffusion phase to a region of very slow spin transport. Throughout this scaling region the charge transport is unaffected. Experiments are discussed in the light of these results, and further experiments to test the theory are proposed.

I. INTRODUCTION

In recent years the description of disordered interacting electronic systems has become a very active field of research. The ultimate goal of this work is to understand both the thermodynamic and transport properties of a disordered Fermi liquid and, in particular, to understand the metal-insulator transition (MIT) such a system presumably undergoes as the strength of the disordered is increased.

The problem of noninteracting disordered electrons is now fairly well understood. A very important step towards our understanding of the pure localization transition (no electron-electron interactions) was Wegner's mapping of that problem onto an effective field theory,[1] which takes the form of a matrix nonlinear σ model.[2] This model yields a lower critical dimension of two for the localization transition, and in $d=2+\epsilon$ dimensions the MIT can be described in terms of an ϵ expansion.

It is clearly desirable to use the same field-theoretic techniques to study the combined effects of disorder and electron-electron interactions. The first contribution in this direction was by Finkelshtein,[3] who mapped the problem onto a nonlinear σ model, corresponding to the noninteracting electrons, and perturbing terms which describe the interactions. Different versions of this model have been studied using renormalization-group (RG) methods.[3-5] The resulting RG flow equations have also been derived from renormalized many-body perturbation theory.[6] Two qualitatively different classes of behavior of the RG flow have been found. If there are magnetic impurities or external magnetic fields, then the RG flow equations predict an interaction driven MIT in $d=2+\epsilon$ dimensions.[4,6] For these cases, the phase transition is a conventional continuous transition and the conductivity exponent extrapolated to three dimensions is unity.

In this paper we consider the general case (no magnetic impurities) where the situation is not so clear. If a RG fixed point exists, it is unconventional in that it occurs at zero disorder and an infinite interaction amplitude such that the product of these two quantities is finite.[7] Within this fixed-point (FP) scenario, one-loop RG calculations imply the following. (i) The above FP is a possibility. (ii) As the FP or phase transition is approached, both the specific heat and the magnetic susceptibility diverge (but with different exponents) while the spin-diffusion coefficient vanishes. (iii) The charge-diffusion coefficient exponent is zero, implying either a discontinuous conductivity or a noncritical conductivity at the phase transition. The latter interpretation implies a separate phase transition before the MIT which involves the spin degrees of freedom. Presumably, for this case, the MIT would occur at larger disorder.

In order for the above scenario to be a viable one, two fundamental questions must be addressed. First, does this unconventional FP exist to all orders? If it does not exist at, say, two-loop order then it cannot be restored at higher order because, as stated above, one of the parameters is flowing to infinity under RG iterations. Second, if the FP exists, does the conductivity exponent remain zero to all orders and if it does, what is the correct interpretation of this?

In this paper we answer both of these questions. We first give a formal proof that to within logarithmic accuracy, the unconventional FP proposed in Ref. 7 exists to all orders in a loop or disorder expansion. We then prove that near this assumed FP, the conductivity exponent s is zero to all orders. Technically, results to "all orders" are

possible because the theory simplifies considerably in the limit where the (triplet) interaction amplitude scales to infinity and the disorder scales to zero. By an explicit two-loop calculation, we then show that logarithmic terms actually suppress the FP. We then interpret what these results imply physically and experimentally. Our main conclusion is that as the MIT is approached from the metallic side a sizable (at least in $d=2+\epsilon$ dimensions) scaling region exists. In this scaling region spin transport slows down dramatically and the magnetic susceptibility and specific heat become large. The equality $s=0$ implies that charge transport does not change appreciably in this scaling region. The regime between this scaling region and the presumed MIT at larger disorder cannot be studied with the techniques used in this paper. The mathematical description of the MIT for the present model thus remains an open problem.

The plan of this paper is as follows. In Sec. II we discuss the basic model, give the Gaussian propagators for the field theory, and give a comprehensive review of the one-loop results. In Sec. III we first formally prove to all orders in a loop expansion that apart from possible logarithmic terms, the RG flow equations have a FP. We then prove that at this FP the conductivity exponent s is zero to all orders in a loop expansion. In Sec. IV we show by explicit calculation that logarithmic terms do appear at two-loop order and suppress the FP discussed in Sec. III. We then derive the effective exponents describing the scaling region in the vicinity of the suppressed FP. In Sec. V we conclude this paper by discussing our results. We will discuss the experimental situation and make some specific experimental predictions that follow from the theory presented here.

Throughout this paper we will assume that the model under consideration is renormalizable with five renormalization constants. Arguments for this to be the case have been presented in Ref. 8. Brief accounts of the work presented here have been given elsewhere.[9,10]

II. THE MODEL AND ONE-LOOP RESULTS

In this section we explain the basic field theory and derive its Gaussian propagators. We review previous results,[3,4,6,8] and extend them by giving the complete one-loop results, which we will need later.

A. The model

For an arbitrary Fermi system the partition function can be written as[11]

$$Z=\int D\bar{\psi}D\psi\exp(S)\ , \tag{2.1a}$$

where the functional integration measure is with respect to anticommuting Grassman fields $\bar{\psi}$ and ψ, and S is the action,

$$S=\int_0^\beta d\tau\int d\mathbf{x}\bar{\psi}^i(\mathbf{x},\tau)\partial_\tau\psi^i(\mathbf{x},\tau)-\int_0^\beta d\tau H'(\tau)\ . \tag{2.1b}$$

Here $H'(\tau)$ is the Hamiltonian in imaginary-time representation, $\beta=T^{-1}$ is the inverse temperature, $i(=1,2)$ denotes spin labels, and summation over repeated spin indices is implied. Our basic model is an electron fluid moving in a static random potential, $V(\mathbf{x})$,

$$H'(\tau)=\int d\mathbf{x}\left[\frac{1}{2m}\nabla\bar{\psi}^i(\mathbf{x},\tau)\cdot\nabla\psi^i(\mathbf{x},\tau)+[V(\mathbf{x})-\mu]\bar{\psi}^i(\mathbf{x},\tau)\psi^i(\mathbf{x},\tau)\right]+\tfrac{1}{2}\int d\mathbf{x}\,d\mathbf{y}\,u(\mathbf{x}-\mathbf{y})\bar{\psi}^i(\mathbf{x},\tau)\bar{\psi}^j(\mathbf{y},\tau)\psi^j(\mathbf{y},\tau)\psi^i(\mathbf{x},\tau)\ . \tag{2.2a}$$

Here m is the particle mass, μ is the chemical potential, and $u(\mathbf{x}-\mathbf{y})$ is the electron-electron interaction potential. We assume that $V(\mathbf{x})$ is δ correlated, and obeys a Gaussian distribution with second moment,

$$\langle V(\mathbf{x})V(\mathbf{y})\rangle=\frac{1}{2\pi N_F\tau}\delta(\mathbf{x}-\mathbf{y})\ , \tag{2.2b}$$

where the angular brackets denote the disorder average, N_F is the bare density of states per spin at the Fermi level, and τ is the bare elastic mean-free time.

All physical (thermodynamic and transport) quantities can be obtained from Eq. (2.1) by adding appropriate source terms to the action. The quenched disorder averages are conveniently performed by means of the replica trick.[12] One introduces N replicas of the system,

$$Z^N=\int D\bar{\psi}D\psi\exp\left[\sum_{\alpha=1}^N S^\alpha\right]\ , \tag{2.3a}$$

with

$$S^\alpha=\sum_n\int d\mathbf{x}\bar{\psi}_n^{\alpha,i}(\mathbf{x})\left[ip_n+\frac{\nabla^2}{2m}+\mu-V(\mathbf{x})\right]\psi_n^{\alpha,i}(\mathbf{x})$$
$$-\frac{T}{2}\sum_{n_1n_2n_3}\int d\mathbf{x}\,d\mathbf{y}\,u(\mathbf{x}-\mathbf{y})\bar{\psi}_{n_1}^{\alpha,i}(\mathbf{x})\bar{\psi}_{n_2}^{\alpha,j}(\mathbf{y})$$
$$\times\psi_{n_3}^{\alpha,j}(\mathbf{y})\psi_{n_1+n_2-n_3}^{\alpha,i}(\mathbf{x})\ . \tag{2.3b}$$

Here $p_n=\pi T(2n+1)$, $n=0,\pm1,\ldots$, is a fermionic Matsubara frequency and the Fourier decomposition,

$$\psi^{\alpha,i}(\mathbf{x},\tau)=(1/\sqrt{\beta})\sum_n\exp[ip_n\tau]\psi_n^{\alpha,i}(\mathbf{x}) \tag{2.3c}$$

has been used. After calculations, the limit $N\to0$ is considered.

Finkelshtein has shown how the field theory for $\langle Z^N\rangle$ can be mapped onto a nonlinear-σ-model-like field

theory.[3] The basic idea is to assume that all of the relevant physics can be expressed in terms of long-wavelength and low-frequency fluctuations of the number density, the spin density, and the single-particle spectral density. Technically this is achieved by repeatedly making long-wavelength approximations and by introducing composite variables that are related to the above fluctuations.

In this paper we do not study the most general Hamiltonian, Eq. (2.2a), but rather introduce two simplifying features. First, we consider the case where the "electron-electron" interaction u is of short range. For the problem studied here this is at least consistent, since our result, a noncritical conductivity, implies that the Coulomb interaction is always screened. Secondly, we neglect the so-called Cooper channel and the associated interference effects which are responsible for localization in the noninteracting case if time reversal symmetry is not violated. There are indications[4] that Cooper pairs may be irrelevant for the MIT in interacting electronic systems. However, the symmetry properties of the interaction term which breaks the symmetry of the underlying nonlinear σ model[8] have never been investigated for the Cooper channel, and we believe that this point warrants further investigation.

The effective Hamiltonian, $H[Q]$, for the composite variable-field theory is

$$H[Q]=\frac{1}{2G}\int d\mathbf{x}\,\mathrm{Tr}[\nabla Q(\mathbf{x})]^2-2H\int d\mathbf{x}\,\mathrm{Tr}[\Omega Q(\mathbf{x})] -\frac{\pi T}{2}(K_t-K_s)\int d\mathbf{x}[Q(\mathbf{x})\cdot Q(\mathbf{x})]_1 +\pi TK_t\int d\mathbf{x}[Q(\mathbf{x})\cdot Q(\mathbf{x})]_2 , \tag{2.4}$$

where to lowest order in the disorder, $G=4/\pi\sigma$, with σ the bare (i.e., self-consistent Born) conductivity. H is a frequency-coupling parameter whose bare value is $H=\pi N_F/2$, and K_t and K_s are triplet and singlet interaction coupling constants, respectively. The field Q is an infinite matrix with complex elements $Q_{nm}^{\alpha\beta,ij}$. Here $\alpha,\beta=1,2,\ldots,N$ are replica indices, $n,m=-\infty,\ldots,+\infty$ are Matsubara frequency indices, and $i,j=1,2$ are spin indices. $\Omega_{nm}^{\alpha\beta,ij}=\delta_{nm}\delta_{\alpha\beta}\delta_{ij}\omega_n$ with $\omega_n=2\pi Tn$ is a bosonic frequency matrix, and Tr denotes a trace over all discrete degrees of freedom. The two "products" in Eq. (2.4) differ in their spin structure and are defined as

$$[Q\cdot Q]_1=\sum_{n_1n_2n_3n_4}\sum_{\alpha}\sum_{ij}\delta_{n_1+n_3,n_2+n_4}Q_{n_1n_2}^{\alpha\alpha,ii}Q_{n_3n_4}^{\alpha\alpha,jj} , \tag{2.5a}$$

$$[Q\cdot Q]_2=\sum_{n_1n_2n_3n_4}\sum_{\alpha}\sum_{ij}\delta_{n_1+n_3,n_2+n_4}Q_{n_1n_2}^{\alpha\alpha,ij}Q_{n_3n_4}^{\alpha\alpha,ji} . \tag{2.5b}$$

The matrix Q is subject to the constraints,

$$Q=Q^+,\quad Q^2=1,\quad \mathrm{Tr}Q=0 . \tag{2.6}$$

These constraints classify Eq. (2.4) as a matrix nonlinear σ model with unitary symmetry, and three perturbing terms. The first one, with coupling constant H, breaks the unitary symmetry and provides an infrared regularization for the model. The other two perturbing terms are due to the electron-electron interactions and they also do not respect the unitary symmetry. The constraints implied by Eq. (2.6) are taken into account by parametrizing the matrix Q by

$$Q=\left[\begin{array}{cc|c} m\geq 0 & m<0 & \\ \hline (1-qq^+)^{1/2} & q & n\geq 0 \\ q^+ & -(1-q+q)^{1/2} & n<0 \end{array}\right] , \tag{2.7}$$

where the q are matrices with complex elements $q_{nm}^{\alpha\beta,ij}$; $n=0,1,\ldots,\ m=-1,-2,\ldots,$. This parametrization[8,13] is the matrix analogon to the elimination of the σ field in the usual vector model.[2] It has a number of technical advantages over other possible parametrizations, most notably it leads to a very transparent loop expansion.

As usual, the explicit elimination of the constraints, Eq. (2.6) by Eq. (2.7) changes the integration measure, which produces additional terms in the effective Hamiltonian if the theory is formulated in terms of the q. However, we choose to use standard field theoretic renormalization procedures.[2] We integrate over all frequencies and use dimensional regularization for the wave-number integrals. With this procedure, the measure terms vanish.

B. The Gaussian theory

To obtain the Gaussian theory we expand Eq. (2.4) in powers of q using Eq. (2.7),

$$H[Q]=H^{(2)}+H^{(3)}+H^{(4)}+\cdots , \tag{2.8}$$

where $H^{(k)}$ is of order q^k. We first concentrate on the Gaussian part of the effective Hamiltonian:

$$H^{(2)}[q]=\frac{1}{G}\int_{\mathrm{p}}\sum_{1,2,3,4}q_{12}(\mathbf{p})M_{12,34}(\mathbf{p})q_{43}^{+}(-\mathbf{p}) . \tag{2.9a}$$

Here $\int_{\mathrm{p}}=\int d\mathbf{p}/(2\pi)^d$ and $1=(n_1,\alpha_1,i_1)$, etc. The matrix $\mathbf{M}$ in Eq. (2.9a) is,

$$M_{12,34}(\mathbf{p})=\delta_{13}\delta_{24}[p^2+GH(\omega_{n_1}-\omega_{n_2})]+\delta_{1-2,3-4}\delta_{\alpha_1\alpha_2}\delta_{\alpha_1\alpha_3}G2\pi T[K_t\delta_{i_1i_3}-\tfrac{1}{2}(K_t-K_s)\delta i_1i_2] . \tag{2.9b}$$

The inverse of the matrix $\mathbf{M}$ determines the Gaussian propagator. Due to the special structure of the nondiagonal part of $\mathbf{M}$, the inversion is easily done. We notice that the inverse of the operator

$$P_{n_1n_2,n_3n_4}=a_{n_1-n_2}\delta_{n_1n_3}\delta_{n_2n_4}+b\delta_{n_1-n_2,n_3-n_4} , \tag{2.10a}$$

has the structure

$$P^{-1}_{n_1 n_2, n_3 n_4} = a^{-1}_{n_1 - n_2} \delta_{n_1 n_3} \delta_{n_2 n_4} + \tilde{b}_{n_1 - n_2} \delta_{n_1 - n_2, n_3 - n_4} \ , \tag{2.10b}$$

and we obtain,

$$\langle q_{12}(\mathbf{p}_1) q^{+}_{43}(\mathbf{p}_2) \rangle^{(2)} = (2\pi)^d \delta(\mathbf{p}_1 + \mathbf{p}_2) \delta_{n_1 - n_2, n_3 - n_4} \delta_{\alpha_1 \alpha_3} \delta_{\alpha_2 \alpha_4} G \times \left[\delta_{n_1 n_3} \delta_{i_1 i_3} \delta_{i_2 i_4} D_{n_1 - n_2}(p_1) + \frac{\delta_{\alpha_1 \alpha_2}}{(n_1 - n_2)} \left[\delta_{i_1 i_3} \delta_{i_2 i_4} \Delta D^{t}_{n_1 - n_2}(p_1) + \frac{\delta_{i_1 i_2} \delta_{i_3 i_4}}{2} \Delta D^{st}_{n_1 - n_2}(p_1) \right] \right] , \tag{2.11}$$

where $\langle \cdots \rangle^{(2)}$ denotes that the average is taken with $H^{(2)}$ only. Here we have introduced the diffusion propagator

$$D_n(p) = (p^2 + GH\omega_n)^{-1} \ , \tag{2.12a}$$

and the singlet and triplet propagators

$$D^{s,t}_n(p) = [p^2 + G(H + K_{s,t})\omega_n]^{-1} \ . \tag{2.12b}$$

In Eq. (2.11) the differences $\Delta D^t \equiv D^t - D$ and $\Delta D^{st} \equiv D^s - D^t$ appear.

C. Results at one-loop order

The RG solution of the model considered here proceeds by first introducing a number of propagators, or equivalently, vertex functions. A loop, or disorder, expansion of each propagator is then generated and the ultraviolet (UV) divergencies of the field theory are found. Renormalization constants are then introduced to make the theory UV finite. These constants can also be used to derive the RG flow equations.

We consider the following propagators:

$$P^{(1)} = \langle Q^{\alpha\alpha, ii}_{nn}(\mathbf{x}) \rangle \ , \tag{2.13a}$$

$$P^{(2)}_0 = \langle q^{\alpha_1 \alpha_2}_n(\mathbf{p}_1) q^{\alpha_1 \alpha_2}_m(\mathbf{p}_2)^* \rangle_{\alpha_1 \neq \alpha_2} \ , \tag{2.13b}$$

$$P^{(2)}_s = \langle q^{\alpha\alpha}_n(\mathbf{p}_1) q^{\alpha\alpha}_m(\mathbf{p}_2)^* \rangle \ , \tag{2.13c}$$

$$P^{(2)}_t = \langle \bar{\mathbf{q}}^{\alpha\alpha}_n(\mathbf{p}_1) \bar{\mathbf{q}}^{\alpha\alpha}_m(\mathbf{p}_2)^* \rangle \ , \tag{2.13d}$$

and the corresponding vertex functions $\Gamma^{(1)}$ and $\Gamma^{(2)}$. Here the averages are to be taken with the full Hamiltonian, and

$$q^{\alpha\beta}_n(\mathbf{p}) = (1/\sqrt{2n}) \sum_{l=1}^{n} \sum_i q^{\alpha\beta, ii}_{n-l, -l}(\mathbf{p}) \ , \tag{2.13e}$$

$$\tilde{\mathbf{q}}^{\alpha\beta}_n(\mathbf{p}) = (1/\sqrt{2n}) \sum_{l=1}^{n} \sum_i (-1)^i q^{\alpha\beta, ii}_{n-l, -l}(\mathbf{p}) \ . \tag{2.13f}$$

For a one-loop calculation of these propagators, it is sufficient to retain terms up to $H^{(4)}$ in Eq. (2.8). The physical meaning of $P^{(1)}$ is that of the one-particle density of states (DOS) at the Fermi level. $P^{(2)}_0$ is the basic diffusion propagator, and $P^{(2)}_s$ and $P^{(2)}_t$ are the charge-density (i.e., singlet) and the spin-density (i.e., triplet) propagators, respectively. From Eqs. (2.12) we see that the bare values of the charge-diffusion constant D_c and the spin-diffusion constant D_s are given by

$$D^{(0)}_c = 1/G(H + K_s) \tag{2.14a}$$

and

$$D^{(0)}_s = 1/G(H + K_t) \ . \tag{2.14b}$$

Similar relations hold for the corresponding renormalized quantities, cf. Eqs. (2.23).

To one-loop order $\Gamma^{(1)}$, or $(P^{(1)})^{-1}$, can be obtained by using Eq. (2.7) to $O(q^2)$ in Eq. (2.13a),

$$\Gamma^{(1)} = 1 + \tfrac{1}{2} \sum_{\alpha_1 i_1 n_1} \langle q^{\alpha\alpha_1, ii_1}_{nn_1}(\mathbf{x}) (q^{+})^{\alpha_1 \alpha, i_1 i}_{n_1 n}(\mathbf{x}) \rangle + O(G^2) \ . \tag{2.15a}$$

With Eq. (2.11), and taking the limit $N \to 0$, we obtain

$$\Gamma^{(1)} = 1 + \frac{G}{4} \sum_{n_1 = -1}^{-\infty} \int_{\mathbf{p}} \frac{1}{(n - n_1)} [3D^t_{n - n_1}(\mathbf{p}) + D^s_{n - n_1}(\mathbf{p}) - 4D_{n - n_1}(\mathbf{p})] + O(G^2)$$

$$= 1 + \frac{\bar{G}}{4\epsilon}(L_s + 3L_t) + O(\epsilon^0 \bar{G}, \bar{G}^2) \ , \tag{2.15b}$$

where we have used dimensional regularization ($\epsilon = d - 2$). Here, and later, the $O(\epsilon^0 \bar{G})$ term will be

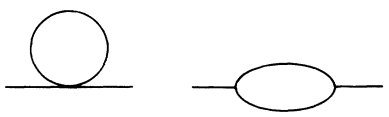

FIG. 1. One-loop diagrams for the two-point vertex functions $\Gamma^{(2)}$.

given when we quote the renormalized vertex functions. In Eq. (2.15b),

$$\bar{G}=S_d G/(2\pi)^d \ , \tag{2.16a}$$

$$L_{s,t}=\ln(1+K_{s,t}/H) \ , \tag{2.16b}$$

where S_d is the surface area of a d-dimensional unit sphere.

To one-loop order, there are two topologically distinct diagrams that contribute to the $\Gamma^{(2)}$ and they are shown in Fig. 1. Tedious but straightforward calculations give

$$\Gamma_0^{(2)}(k,m)=k^2/G+H\omega_m+\Delta\Gamma_0^{(2)}(k,m) \ , \tag{2.17a}$$

with

$$\Delta\Gamma_0^{(2)}(k,m)=(k^2+GH\omega_m)\int_{\mathbf{p}}[I_1^s(\mathbf{p})+3I_1^t(\mathbf{p})] - G\omega_m\int_{\mathbf{p}}[K_s I_2^s(\mathbf{p})+3K_t I_2^t(\mathbf{p})]$$
$$\simeq\delta\Gamma_s^{(2)}+3\delta\Gamma_t^{(2)} \ , \tag{2.17b}$$

$$\Gamma_s^{(2)}(k,m)=k^2/G+(H+K_s)\omega_m+\Delta\Gamma_s^{(2)}(k,m) \ , \tag{2.17c}$$

with

$$\Delta\Gamma_s(k,m)=(k^2+GH\omega_m)\int_{\mathbf{p}}[I_1^s(\mathbf{p})+3I_1^t(\mathbf{p})]-G\omega_m(K_s+3K_t)\int_{\mathbf{p}}J_1(\mathbf{p})$$
$$-G\omega_m\int_{\mathbf{p}}[K_s\tilde{I}_2^s(\mathbf{p})+3K_t\tilde{I}_2^t(\mathbf{p})]-G\omega_m K_s\int_{\mathbf{p}}J_2(\mathbf{p})$$
$$\simeq\delta\Gamma_s^{(2)}+3\delta\Gamma_t^{(2)}+\frac{\bar{G}}{4\epsilon}\omega_m(K_s+3K_t)+\frac{\bar{G}}{2\epsilon}\omega_m K_s(L_s+3L_t) \ , \tag{2.17d}$$

and

$$\Gamma_t^{(2)}(k,m)=k^2/G+(H+K_t)\omega_m+\Delta\Gamma_t^{(2)}(k,m) \ , \tag{2.17e}$$

with

$$\Delta\Gamma_t^{(2)}(k,m)=(k^2+GH\omega_m)\int_{\mathbf{p}}[I_1^s(\mathbf{p})+3I_1^t(\mathbf{p})]+G\omega_m(K_t-K_s)\int_{\mathbf{p}}J_1(\mathbf{p})$$
$$-G\omega_m\int_{\mathbf{p}}[K_s\tilde{I}_2^s(\mathbf{p})+3K_t\tilde{I}_2^t(\mathbf{p})]-G\omega_m K_t\int_{\mathbf{p}}J_3(\mathbf{p})$$
$$\simeq\delta\Gamma_s^{(2)}+3\delta\Gamma_t^{(2)}+\frac{\bar{G}}{4\epsilon}\omega_m(K_s-K_t)-\frac{\bar{G}}{\epsilon}\omega_m(K_t^2/H)+\frac{\bar{G}}{2\epsilon}\omega_m K_t(L_s+3L_t) \ . \tag{2.17f}$$

The integrands in Eqs. (2.17b), (2.17d), and (2.17f) are given explicitly in the appendix. Their evaluation to leading terms in $1/\epsilon$ yields the results quoted earlier, with

$$\delta\Gamma_{s,t}^{(2)}=\frac{(k^2/G)\bar{G}}{2\epsilon}\left[1-\frac{H}{K_{s,t}}L_{s,t}\right] +\omega_m\frac{\bar{G}H}{2\epsilon}\left[L_{s,t}-\frac{K_{s,t}}{2H}\right] \ . \tag{2.17g}$$

Note that the factor $\bar{G}/G$ in the first term of Eq. (2.17g) serves only to absorb the factor $S_d/(2\pi)^d$ arising from the momentum integration.

The typical logarithmic structure in all of these functions arises from performing the summation over frequencies. One way to do the integrals is to perform the wave-number integration first, and then to express the sums over the Matsubara indices in terms of Riemann ζ functions. The pole structure of the latter gives rise to divergencies for $\epsilon\to 0$. Alternatively, one can transform the Matsubara frequency sums to real frequency integrals using standard methods. The pole in ϵ then arises from the subsequent integration over wave numbers. Notice that both diagrams in Fig. 1 contribute terms which individually are linearly divergent in $d=2$. In Eqs. (2.17) we have combined terms in such a way that these "superdivergencies" cancel.

We next absorb the ultraviolet divergencies (here the singularities as $\epsilon\to 0$) encountered in the theory, Eqs. (2.15)–(2.17), into renormalization constants. The question of whether or not this model is renormalizable in general has been discussed elsewhere.[8] We define a renormalized disorder coupling constant g, a renormalized frequency coupling constant h, and renormalized interaction constants k_s, k_t by

$$\bar{G}=\kappa^{-\epsilon}Z_1 g \ , \tag{2.18a}$$

$$H=Z_H h \ , \tag{2.18b}$$

$$K_{s,t}=Z_{s,t}k_{s,t} \ , \tag{2.18c}$$

where κ is an arbitrary momentum scale. The renormalization statement is

$$\Gamma_R^{(N)}(p,m;g,h,k_s,k_t,\kappa)=Z^{N/2}\Gamma^{(N)}(p,m;G,H,K_s,K_t) \ , \tag{2.19}$$

where $\Gamma_R^{(N)}$ is the renormalized vertex function and Z is the field renormalization constant. The four functions $\Gamma^{(1)}$ and $\Gamma_{0,s,t}^{(2)}$ are sufficient to determine the five renormalization constants. Using minimal subtraction and

Eqs. (2.15)–(2.19) we find

$$Z=1-\frac{g}{2\epsilon}(l_s+3l_t)+O(g^2)\ , \tag{2.20a}$$

$$Z_1=1+\frac{g}{2\epsilon}\{[1-(1+h/k_s)l_s] +3[1-(1+h/k_t)l_t]\}+O(g^2)\ , \tag{2.20b}$$

$$Z_H=1+\frac{g}{4\epsilon h}(k_s+3k_t)+O(g^2)\ , \tag{2.20c}$$

$$Z_s=1-\frac{g}{4\epsilon}(1+3k_t/k_s)+O(g^2)\ , \tag{2.20d}$$

and

$$Z_t=1+\frac{gk_t}{\epsilon h}+\frac{g}{4\epsilon}(1-k_s/k_t)+O(g^2)\ , \tag{2.20e}$$

where $l_{s,t}=\ln(1+k_{s,t}/h)$.

The one-loop RG flow equations follow from Eqs. (2.18) and (2.20) in the usual way. With $b\sim\kappa^{-1}$, the RG length scale factor, we obtain

$$b\frac{dg}{db}=-\epsilon g+\frac{g^2}{2}[4-3(1+h/k_t)l_t -(1+h/k_s)l_s]+O(g^3)\ , \tag{2.21a}$$

$$b\frac{dh}{db}=\frac{g}{4}[k_s+3k_t]+O(g^2)\ , \tag{2.21b}$$

$$b\frac{d}{db}[h+k_s]=0\ , \tag{2.21c}$$

and

$$b\frac{dk_t}{db}=g\frac{k_t^2}{h}+g\frac{k_t}{4}-\frac{g}{4}k_s+O(g^2)\ . \tag{2.21d}$$

For future use we define $\gamma_t\equiv k_t/h$, which obeys

$$b\frac{d\gamma_t}{db}=\frac{g\gamma_t^2}{4}+\frac{g\gamma_t}{4}\left[1-\frac{k_s}{h}\right]-\frac{g}{4}\frac{k_s}{h}+O(g^2)\ . \tag{2.21e}$$

Let us now emphasize a few points.

(1) Equation (2.21c) implies that to one-loop order the sum $h+k_s$ is not renormalized. This result is expected to be exact. The basic idea is that because $h+k_s$ multiplies the frequency factor in the hydrodynamic poles for density diffusion it can be related to the density compressibility χ_n, or the thermodynamic DOS. This quantity is expected to be insensitive to diffusion corrections.[3] We note that if χ_n was singular, then charge and mass transport would be qualitatively different according to an Einstein relation. Physically, and in agreement with the one-loop results, this seems unlikely.

(2) Equations (2.21b) and (2.21c) imply that both h and $|k_s|$ increase under RG iterations such that $k_s/h\to-1$. In this limit Eqs. (2.21), for the short-range electron-electron interaction model, reduce[6] to the one-loop equations for the case of electrons interacting via a Coulomb potential.

(3) Examining Eqs. (2.21) one sees that there is a nontrivial fixed point at $g\to0$, $\gamma_t\to\infty$ such that $y=g\gamma_t$ is finite.[7] In this limit $k_s/h=-1$ and the RG flow equations are

$$b\frac{dg}{db}=-\epsilon g+O(g^3)\ , \tag{2.22a}$$

$$b\frac{dh}{db}=\tfrac{3}{4}yh+O(g^2)\ , \tag{2.22b}$$

$$b\frac{d\gamma_t}{db}=\frac{y}{4}\gamma_t+O(g^2)\ , \tag{2.22c}$$

and

$$b\frac{dy}{db}=-\epsilon y+\frac{y^2}{4}+O(g^3)\ . \tag{2.22d}$$

Equations (2.22) do have a nontrivial FP at $g^*=0$, $\gamma_t^*=\infty$, and $y^*=g^*\gamma_t^*=4\epsilon$. Linearization of Eq. (2.22d) around this FP leads to a RG relevant eigenvalue that gives the inverse correlation length exponent $\nu=1/\epsilon+O(1)$.

The above FP has several interesting aspects. For example, g is a dangerous irrelevant variable as far as the diffusion coefficients are concerned because they diverge as $g\to0$. Let us consider the renormalized charge- and spin-diffusion coefficients. They read [cf. Eqs. (2.14)] as

$$D_c\sim b^{-\epsilon}/g(h+k_s) \tag{2.23a}$$

and

$$D_s\sim b^{-\epsilon}/g(h+k_t)=b^{-\epsilon}/h(g+y)\ . \tag{2.23b}$$

In the renormalized spin-diffusion coefficient, Eq. (2.23b), the divergences of $1/g$ and γ_t cancel, and the divergence of h as well as the factor of $b^{-\epsilon}$ drive D_s towards zero. For the charge-diffusion coefficient D_c, or conductivity σ, the situation is less clear. Because the time scale in the singlet channel $h+k_s$ is not renormalized, D_c at zero frequency and zero temperature satisfies the scaling law

$$D_c(\delta y,g)=b^{-\epsilon}D_c(b^{1/\nu}\delta y,b^{-\theta}g)\ . \tag{2.24a}$$

Here $\theta=\epsilon+O(\epsilon^2)$ is the scaling dimension of g, δy is the deviation of y from its FP value, and the $b^{-\epsilon}$ factor arises because D_c has the dimensions of a length squared ($\sim b^2$) divided by a time scale ($\sim b^d$). In giving Eq. (2.24a) we have consistently (with the existence of a FP) assumed that D_c depends on γ_t only through the combination y. Choosing $b\sim(\delta y)^{-\nu}$ and using $D_c(g\to O)\sim g^{-1}$, we obtain

$$D_c\sim\sigma\sim(\delta y)^s\ , \tag{2.24b}$$

$$s=\nu(\epsilon-\theta)\ . \tag{2.24c}$$

Equations (2.24) also follow directly from Eq. (2.23a). Note that if the thermodynamical DOS were critical, then D_c and σ would have different exponents, but the conductivity exponent would still be given by Eq. (2.24c). This follows from an Einstein relation which states that σ and D_c are identical apart from a thermodynamic DOS. Equation (2.24c) is a generalization of Wegner's scaling law for noninteracting electrons.[14] In the absence of interactions, g has a nonzero FP value and $s=\nu\epsilon$. Here, the one-loop calculation, Eq. (2.22a), yields $\theta=\epsilon+O(\epsilon^2)$

so that $s=O(\epsilon)$. The one-loop result thus suggests the possibility that $s=0$. As already mentioned *a priori*, a zero exponent can imply either a discontinuous conductivity or a noncritical conductivity.

Taking an alternative viewpoint, we note that near the proposed FP, all one-loop renormalizations of the singlet channel vanish. This is consistent with a noncritical conductivity and with the idea that the mass diffusion is decoupled and not affected by the anomalies that seem to be happening in the diffusion channel $\Gamma_0^{(2)}$ and spin-diffusion (magnetic) channel $\Gamma_t^{(2)}$. These anomalies will be discussed later.

Finally, we use Eqs. (2.17)–(2.20) to determine the renormalized vertices, $\Gamma_R^{(1)}$ and $\Gamma_{o,s,t,R}^{(2)}$, to $O(\epsilon^0 g)$ near the fixed point discussed earlier. We obtain (here we put $\kappa=1$),

$$\Gamma_R^{(1)} \simeq 1+O(g^2) , \tag{2.25a}$$

$$\Gamma_{0,R}^{(2)}(p,m) \simeq \frac{1}{g}[(p^2/G)\bar{G}+gh\omega_m]-h\omega_m \tfrac{3}{8} g\gamma_t\{-\tfrac{3}{2}+\ln[gh\omega_m(1+\gamma_t)]\}+O(\epsilon) , \tag{2.25b}$$

$$\Gamma_{s,R}^{(2)}(p,m) \simeq \frac{1}{g}[(p^2/G)\bar{G}+g(h+k_s)\omega_m]+(\text{two-loop-order terms}) , \tag{2.25c}$$

$$\Gamma_{t,R}^{(2)}(p,m) \simeq \frac{1}{g}[(p^2/G)\bar{G}+g(h+k_t)\omega_m]-k_t\omega_m \frac{g\gamma_t}{2}[-1+\pi^2/48+\tfrac{1}{4}(\ln 2)^2+\ln(gh\omega_m)-\tfrac{1}{2}(\ln 2)l_s]+O(\epsilon) . \tag{2.25d}$$

Two things should be noted. First, near the FP, $\Gamma^{(1)}$ and $\Gamma_s^{(2)}$ have no renormalizations and are essentially decoupled from the physics associated with the RG equations (2.21). Note that the complete absence of one-loop-order terms in Eq. (2.25c) is due to nontrivial cancellation of various terms in Eq. (2.17d). This cancellation to all orders in ϵ is an indication that $h+k_s$ is indeed, as assumed earlier, not renormalized at any order of the loop expansion. Second, the vertex functions $\Gamma_{0,R}^{(2)}$ and $\Gamma_{t,R}^{(2)}$ have renormalized "logarithmic" contributions with different frequency or time scales. This suggests a violation of strong dynamical scaling,[15] which in turn suggests that the proposed FP is problematic. We will return to this point later.

III. FORMAL PROOF OF THE EXISTENCE OF A FIXED POINT AND OF $s=0$

In this section we first prove that except for possible logarithmic problems, the FP discussed in Sec. II exists to all orders in a disorder or loop expansion. Near this assumed FP, we then prove that the conductivity exponent s, is zero to all orders in a loop expansion.

A. Existence of a fixed point

At higher than one-loop order, the existence of the FP discussed in Sec. II is not obvious. If for $\gamma_t \to \infty$ a term of order g^n grows like γ_t^p with $p>n-1$ in Eq. (2.22a), or $p>n$ in Eq. (2.22b), or $p>n+1$ in Eq. (2.22c), then the FP scenario breaks down. In fact, it is easy to find diagrammatic contributions that *appear* not to be consistent with the FP scenario. For example, the diagram in Fig. 2 would seem to lead to a scenario violating term of order $g^3\gamma_t^4$ in Eq. (2.22a) because it involves four q^3 "interacting" vertices that according to Eqs. (2.4), (2.5), and (2.7) can each be of $O(K_t)$. Note that here and elsewhere, K_t must appear in the combination $K_t/H[\sim O(\gamma_t)]$ for dimensional reasons. Moreover, here, and below, we do not distinguish between K_t or H and the respective renormalized quantities, k_t or h, because ultimately the latter appear in the theory.

To prove that the FP scenario is a possibility, we start

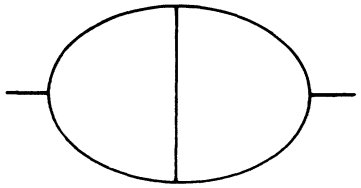

FIG. 2. A two-loop contribution to $\Gamma^{(2)}$ which according to naive power counting is of order K_t^4.

with the expansion indicated by Eq. (2.8). A diagrammatic perturbation theory for the model thus contains vertices with an arbitrary number of q fields or "free lines." The vertices with an odd number of q fields always carry an interaction amplitude or coupling constant. The vertices with an even number of q fields may or may not carry an interaction amplitude. Inspection of Eq. (2.8) shows that all odd vertices contain a factor

$$V_{\text{odd}} \sim \sum_{n_3 n_4} \sum_{i_3 i_4} \delta_{n_2 - n_1, n_3 - n_4} [K_t \delta_{i_3 i_2} \delta_{i_4 i_1} + \tfrac{1}{2}(K_s - K_t)\delta_{i_1 i_2}\delta_{i_3 i_4}] q^{\alpha\alpha, i_3 i_4}_{n_3 n_4} , \tag{3.1}$$

where n_3, n_4 and i_3, i_4 appear *only* in the above term. V_{odd} (and, in particular, V_3) plays a central role in the theory because at l-loop order in the perturbation theory there exists a diagram with $2l$ V_3 vertices and this diagram has the maximum number (at fixed l) of K_t factors (using naive counting). The term shown in Eq. (3.1) is the only element appearing in the vertices which is diagonal in replica space. It plays an important role in the diagrammatic analysis. We denote it by a broken line, and all other q's by solid lines. Each odd vertex of order $2n+1$ then has $2n$ solid lines emanating from it, and one broken line. Because replica labels must match under Gaussian contractions [cf. Eq. (2.11)], we can say that contractions of broken lines with solid lines yield broken lines.

We will now explore some general properties of the diagrams appearing in the loop expansion. Let us consider an arbitrary diagram contributing to a two-point vertex function. Suppose the diagram contains n vertices with a total number (before contraction) of m free lines. Elementary combinatorics shows that the number of loops in the diagram is

$$l = (m - 2n)/2 . \tag{3.2}$$

We are interested in the behavior of the diagram for $K_t \to \infty$ (or $\gamma_t \to \infty$). Except for some special cases, which we discuss below, it goes like K_t^p, where p is the number of interaction amplitude carrying vertices minus the number of reductions due to (i) singlet rather than triplet amplitudes or (ii) triplet propagators which behave like K_t^{-1} for large K_t. We will use the following.

Lemma. Internal broken lines with different frequency-momentum reduce the order in K_t of the diagram by one each. n broken lines with the same frequency-momentum always occur in such a way that they reduce the order by either $n-1$ or n.

Proof. Contraction of the q field in Eq. (3.1) with an arbitrary other q field produces a Gaussian propagator consisting of two terms with different spin structure [cf. Eq. (2.11)]. One leads to a singlet amplitude K_s by means of the term in square brackets in Eq. (3.1). The other has a contribution proportional to K_t, but its frequency structure yields a triplet propagator. Independent triplet propagators lead to a factor K_t^{-1} upon frequency integration. With all frequency factors taken into account, a product of n identical triplet propagators leads to a factor of either $K_t^{-(n-1)}$ or K_t^{-n} upon integration.

This final point deserves further discussion. There are two cases to consider and they both involve propagator renormalizations in skeleton diagrams. In the first case the original (bare) triplet propagator does not arise from the factor given by Eq. (3.1), but instead arises from an even vertex. This diagram and its propagator renormalizations are shown in Fig. 3. Now, in general, there is a factor (frequency)$^{-1}$ from the prefactor of D^t in Eq. (2.11). The largest (as $K_t \to \infty$) term in each of the bubbles in Fig. 3(b) is from a renormalization of K_t (frequency) in D^t. Therefore, if there are n identical propagators then there are $n-2$ factors of frequency. Integration over frequency then gives a factor $K_t^{-(n-1)}$. In the second case the original triplet propagator does arise from the factor given by Eq. (3.1). In this case, the frequency sums [n_3, n_4 in Eq. (3.1)] provide an additional frequency factor in the numerator. Integration over frequency for this case gives a factor K_t^{-n}.

We now consider the soft and triplet two-point vertex functions $\Gamma_0^{(2)}$ and $\Gamma_t^{(2)}$ in the limit of large K_t. As explained earlier, their dependence on K_t is of central importance for the existence or otherwise of the FP at $\gamma_t \to \infty$. We now prove the following.

Theorem. For $K_t \to \infty$, no l-loop contribution to $\Gamma_0^{(2)}$ diverges more strongly than K_t^p with $p \le l$.

Proof. Let there be n vertices with m free lines. Let n_0 of the vertices be odd and $n_e = n - n_0$ of the vertices be even; then $m \ge 3n_0 + 4n_e$. With Eq. (3.2) we have $l \ge n_e + n_0/2$. Now $p \le n - n_r$, where n_r is the number of singlet amplitudes and triplet propagators reducing p. $\Gamma_0^{(2)}$ has no external broken lines. Assume first that there are no broken lines carrying the same frequency momen-

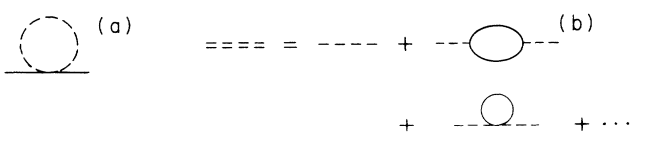

FIG. 3. (a) A relevant diagram that is not generated by interacting vertices. (b) Renormalization of the triplet propagator (dashed line) in (a).

tum. Then $n_r \geq n_0/2$ according to the lemma. Therefore, $p \leq n - n_0/2 = n_e + n_0/2 \leq l$. Next assume there are r identical broken lines. If they all arise from Eq. (3.1) then $n_r \geq n_0/2$ according to the lemma and again $p \leq l$. If they do not all arise from Eq. (3.1) then two of the broken lines must be attached to the same (even) vertex. Consequently, the broken lines are not maximally contracted and their number is $n_b \geq n_0/2+1$. The lemma yields $n_r \geq n_b - 1 \geq n_0/2$, so again $p \leq l$. If there are both a number of independent triplet propagators and a number of identical triplet propagators in a particular diagram, then a combination of the aforementioned arguments again leads to $p \leq l$.

Theorem. For $K_t \to \infty$ no l-loop contribution to $\Gamma_t^{(2)}$ diverges more strongly than K_t^p with $p \leq l+1$.

Proof. The proof is identical to that for the above theorem except that $\Gamma_t^{(2)}$ has two external broken lines. For this case $n_r \geq (n_0-2)/2 = n_0/2-1$. Therefore, $p \leq n - (n_0/2)+1 = n_e + (n_0/2)+1 \leq l+1$.

An analogous argument proves that no l-loop contribution to $\Gamma^{(1)}$ diverges more strongly than K_t^p with $p \leq l-1$. Going through the renormalization procedure, given in Sec. II, at l-loop order we see that these conditions allow for a RG fixed point where $g \to 0$, $\gamma_t \to \infty$ such that $y = g\gamma_t$ is finite. The result for $\Gamma^{(1)}$ implies that the density of states is uncritical at this FP.

Following these formal proofs, let us emphasize a few points and caveats.

(1) In giving the above estimates we have assumed that all factors of K_t are generated by the interacting nonlinearities in Eq. (2.8) and that the nonlinearities that are present in the absence of interactions are irrelevant in the $g \to 0$, $\gamma_t \to \infty$ limit; this is not correct. These nonlinearities are proportional to either a momentum squared or a frequency. When these factors multiply a triplet propagator and when dimensional regularization is used, a factor K_t in the numerator can result. Effectively, the relevant momentum region scales like $K_t^{1/2}$ and the momentum-squared factor gives a K_t. These contributions, however, do *not* invalidate the above theorems. Namely, all of the noninteracting vertices in Eq. (2.8) are even vertices. At l-loop order there can at most be l of these vertices in a diagram for $\Gamma^{(2)}$. Therefore, these contributions are at most of order K_t^l.

(2) The arguments given in the "proofs" assume that the $K_t \to \infty$ limit can be taken before summation over internal frequencies and integrals over internal wave numbers are performed. In general, this is not correct. We know that the integrals are logarithmically divergent in two dimensions and that they diverge as ϵ^{-1} in $d = 2+\epsilon$ dimensions when dimensional regularization is used. Simple examples show that these "logarithmic" divergencies imply that depending on how the limit $K_t \to \infty$ is taken, either a $1/\epsilon$ or a $\ln\gamma_t$ can be obtained.

(3) Logarithmic problems of a different kind might be expected from an inspection of the renormalized triplet vertex, Eq. (2.25d). The latter contains a term proportional to $l_s = \ln[(h+k_s)/h]$ which is of maximum possible order in k_t. Upon insertion in lower-order graphs, this term might produce leading terms (as $k_t \to \infty$) proportional to l_s at two-loop and higher order. Such contributions would violate the conditions for the FP, since near the FP, $h \to \infty$ while $h + k_s$ remains constant, and hence, $l_s \to -\infty$ [cf. Eqs. (2.21c) and (2.22b)].

We conclude that our proof of the existence of a FP is uncertain due to possible logarithmic problems. It is clear, however, that even if these terms exist, they will become important only extremely close to the proposed FP. It will therefore be very useful to know the critical behavior, even if it should finally turn out that the logarithmic terms do pose a problem. Before we come back to the logarithms, we therefore consider the conductivity exponent.

B. The conductivity exponent

Here we prove to all orders that near the assumed FP the conductivity exponent s is identically equal to zero. Technically, we show that the exponent θ, defined by Eqs. (2.24), is equal to ϵ. Elsewhere we showed this to two-loop order by explicit calculation.[9] Here we give the general "proof."

We are interested only in the leading terms in the $g \to 0$, $\gamma_t \to \infty$ limit. It follows from the proof of the theorems in Sec. III A that we can truncate the effective Hamiltonian at order q^4. To see this note that in the proof we used $m \geq 3n_o + 4n_e$ because the leading odd vertex is $\sim q^3$ and the leading even vertex is $\sim q^4$. Diagrams with higher-order vertices satisfy $m \geq 3n_o + 4n_e + 2\delta$ with δ a positive integer. These diagrams lead to terms of order K_t^p with $p \leq l - \delta$ for $\Gamma_0^{(2)}$ and $p \leq l+1-\delta$ for $\Gamma_t^{(2)}$. They are therefore irrelevant. To order q^4 the effective Hamiltonian is written as

$$H = H^{(2)} + H^{(3)} + H_0^{(4)} + H_I^{(4)} . \tag{3.3}$$

Here $H_0^{(4)}$ is the quartic term that exists in the field theory in the absence of interaction effects and $H_I^{(4)}$ is the quartic term due to the interactions. The interaction nonlinearities play a special role and from Eqs. (2.4), (2.5), (2.7), and (3.3) they are given explicitly by

$$H^{(3)} = -\pi T \sum_{(\alpha,n,i)} \int d\mathbf{x} \delta_{n_2-n_1,n_3-n_4} [K_t \delta_{i_3 i_2} \delta_{i_4 i_1} + \tfrac{1}{2}(K_s - K_t)\delta_{i_1 i_2}\delta_{i_3 i_4}] \times [q_{n_1 n_5}^{\alpha_1\alpha_2, i_1 i_5} (q_{n_2 n_5}^{\alpha_1\alpha_2, i_2 i_5})^* - (q_{n_5 n_1}^{\alpha_2\alpha_1, i_5 i_1})^* q_{n_5 n_2}^{\alpha_2\alpha_1, i_5 i_2}][q_{n_3 n_4}^{\alpha_1\alpha_1, i_3 i_4} + (q_{n_4 n_3}^{\alpha_1\alpha_1, i_4 i_3})^*] \tag{3.4a}$$

and

$$H_I^{(4)}=\frac{\pi T}{4}\sum_{\{\alpha,n,i\}}\int d\mathbf{x}\,\delta_{n_2-n_1,n_3-n_4}[K_t\delta_{i_3i_2}\delta_{i_4i_1}+\tfrac{1}{2}(K_s-K_t)\delta_{i_1i_2}\delta_{i_3i_4}][q_{n_1n_5}^{\alpha_1\alpha_2,i,i_5}(q_{n_2n_5}^{\alpha_1\alpha_2,i_2i_5})^*-(q_{n_5n_1}^{\alpha_2\alpha_1,i_5i_1})^*q_{n_5n_2}^{\alpha_2\alpha_1,i_5i_2}]$$
$$\times[q_{n_3n_6}^{\alpha_1\alpha_3,i_3i_6}(q_{n_4n_6}^{\alpha_1\alpha_3,i_4i_6})^*-(q_{n_6n_3}^{\alpha_3\alpha_1,i_6i_3})^*q_{n_6n_4}^{\alpha_3\alpha_1,i_6i_4}]\ . \tag{3.4b}$$

The exponent θ determines the disorder renormalization and it can be determined by calculating any of the two-point propagators given by Eqs. (2.13). We choose to consider the off-diagonal (in replica space) propagator,

$$P_0^{(2)}(k,m)=\langle q_m^{\alpha_1\alpha_2}(\mathbf{k})q_m^{\alpha_1\alpha_2}(\mathbf{k})^*\rangle_c^H(1-\delta_{\alpha_1\alpha_2})\ , \tag{3.5a}$$

where $\langle\cdots\rangle_c^H$ denotes an average with weight $\exp[-H]$, where only connected diagrams are considered. In the Gaussian approximation (denoted by an index G), Eq. (3.5a) is given by

$$P_{0,G}^{(2)}(k,m)=V[k^2/G+H\omega_m]^{-1}\ , \tag{3.5b}$$

where V is the system volume. The renormalization of G in Eq. (3.5b) by the non-Gaussian terms in Eq. (3.3) determines θ. We next argue that near the proposed FP, all renormalizations of G either vanish or cancel. Therefore, g has its bare dimension ϵ, which implies $\theta=\epsilon$ exactly.

In Sec. III A it was shown that in the perturbation theory for $P_0^{(2)}$, the diagonal (in replica space) q fields in the last term in (3.4a) must be maximally contracted together to yield a nonvanishing contribution to the renormalization of G at the FP. This implies we can expand in powers of $H^{(3)}$ (only even powers appear),

$$P_0^{(2)}(k,m)=\left\langle q_m^{\alpha_1\alpha_2}(\mathbf{k})q_m^{\alpha_1\alpha_2}(\mathbf{k})^*\sum_{n=0}^{\infty}\frac{1}{(2n)!}(H^{(3)})^{2n}\right\rangle_c^{H^{(2)}+H^{(4)}}, \tag{3.6a}$$

and contract the diagonal q fields in $(H^{(3)})^{2n}$ even though the Hamiltonian $H^{(2)}+H^{(4)}$ is not Gaussian. There are $(2n-1)!!=(2n-1)!/2^{n-1}(n-1)!$ independent such contractions in $(H^{(3)})^{2n}$, and, as a result, Eq. (3.6a) can be written as

$$P_0^{(2)}(k,m)=\langle q_m^{\alpha_1\alpha_2}(\mathbf{k})q_m^{\alpha_1\alpha_2}(\mathbf{k})^*\rangle_c^{H^{(2)}+H_0^{(4)}+H_{I,\mathrm{eff}}^{(4)}}\ . \tag{3.6b}$$

Here $H_{I,\mathrm{eff}}^{(4)}$ is an effective quartic term due to the interactions. It consists of $H_I^{(4)}$ and a term generated by reexponentiating the partially contracted factors $(H^{(3)})^{2n}$ in Eq. (3.6a) [if the last term in Eq. (3.4a) is contracted, then the remaining part of $(H^{(3)})^2$ is of order q^4]. Neglecting irrelevant singlet contributions, $H_{I,\mathrm{eff}}^{(4)}$ can be written in momentum space as

$$H_{I,\mathrm{eff}}^{(4)}=\frac{\pi T}{4}\sum_{\{\alpha,n,i\}}\int_{\mathbf{p}_1,\ldots,\mathbf{p}_4}\delta_{n_2-n_1,n_3-n_4}(2\pi)^d\delta(\mathbf{p}_1+\mathbf{p}_2+\mathbf{p}_3+\mathbf{p}_4)[K_t\delta_{i_3i_2}\delta_{i_4i_1}+\tfrac{1}{2}(K_s-K_t)\delta_{i_1i_2}\delta_{i_3i_4}]\Delta(\mathbf{p}_1+\mathbf{p}_2,|\mathbf{n}_2-\mathbf{n}_1|)$$
$$\times[q_{n_1n_5}^{\alpha_1\alpha_2,i_1i_5}(\mathbf{p}_1)q_{n_2n_5}^{\alpha_1\alpha_2,i_2i_5}(\mathbf{p}_2)^*-q_{n_5n_1}^{\alpha_2\alpha_1,i_5i_1}(\mathbf{p}_1)^*q_{n_5n_2}^{\alpha_2\alpha_1,i_5i_2}(\mathbf{p}_2)]$$
$$\times[q_{n_3n_6}^{\alpha_1\alpha_3,i_3i_6}(\mathbf{p}_3)q_{n_4n_6}^{\alpha_1\alpha_2,i_4i_6}(\mathbf{p}_4)^*-q_{n_6n_3}^{\alpha_3\alpha_1,i_6i_3}(\mathbf{p}_3)^*q_{n_6n_4}^{\alpha_3\alpha_1,i_6i_4}(\mathbf{p}_4)] \tag{3.7a}$$

with

$$\Delta(\mathbf{p}_1+\mathbf{p}_2,|n_2-n_1|)=1-\frac{K_t|\omega_{n_2}-\omega_{n_1}|}{[(\mathbf{p}_1+\mathbf{p}_2)^2/G+(K_t+H)|\omega_{n_2}-\omega_{n_1}|]}\ . \tag{3.7b}$$

The triplet propagator in Eq. (3.7b) arises from the contraction of the diagonal q fields in Eq. (3.4a).

The nonlinearity in the effective Hamiltonian for $P_0^{(2)}$ is now $H_{\mathrm{NL}}=H_0^{(4)}+H_{I,\mathrm{eff}}^{(4)}$. Using

$$\lim_{K_t\to\infty}\Delta(\mathbf{p}_1+\mathbf{p}_2,|n_2-n_1|)=0\ ,$$

we formally conclude that H_{NL} is of order $(K_t)^0$. This implies that G is not renormalized near the $g\to0$, $\gamma_t\to\infty$ FP and that the renormalized disorder is simply $g=b^{-\epsilon}G$. This formally proves $\theta=\epsilon$ and $s=0$.

The argument given above assumes that in Eq. (3.7b) the limit $K_t\to\infty$ can be taken before summations over internal frequencies and integrals over internal wave numbers are performed. As already mentioned in Sec. III A, in some situations this is problematic. For example, the aforementioned arguments seem to imply that the frequency-coupling constant H in Eq. (3.5b) is not renormalized near the $g\to0$, $\gamma_t\to\infty$ FP. The explicit one-loop calculations given in Sec. II and elsewhere show that such a conclusion is not correct. Equation (2.17b) shows that in the perturbation theory for $P_0^{(2)}(k,m)$ (or $\Gamma_0^{(2)}$), finite-frequency sums occur with an upper limit of ω_m. For these terms the general arguments are in error since

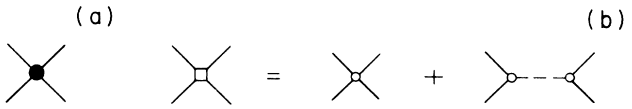

FIG. 4. (a) The quartic vertex which would be present even in the absence of electron-electron interactions is represented by a solid circle. (b) Interacting four-point vertex in the effective theory and equivalent vertices in the original theory. Open circles denote interacting vertices in the original theory.

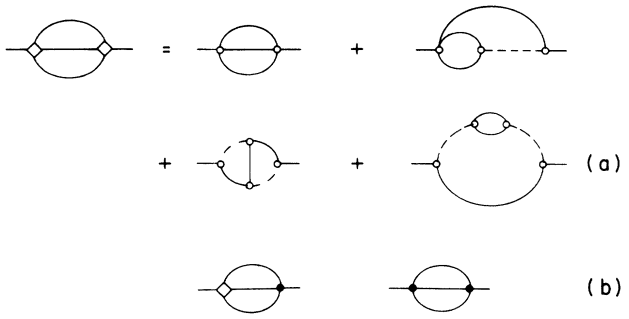

FIG. 5. (a) Two-loop skeleton diagram in the effective theory. Also shown are the diagrams in the original theory. (b) Two-loop skeletons which do not contribute near the proposed FP.

$K_t \to \infty$ does not commute with doing the integrals. In the calculation of the G renormalization [related to the k^2 term in Eq. (3.5b) rather than the ω_m term] this "accident" does not occur since power counting shows that these finite-frequency sums necessarily result in terms that are either UV finite or are irrelevant in the long-wavelength and small-frequency limit.

There are a number of other accidents which prevent the naive interpretation that $H^{(4)}_{I,\text{eff}}$ is of order $(K_t)^0$, in general. These points are most easily discussed after we have explicitly done the two-loop calculation for the H and K_t renormalizations. Our eventual conclusion is that none of these diagrammatic accidents invalidate our $s=0$ result, and we will present the arguments for this in Sec. IV.

IV. BREAKDOWN OF THE FIXED-POINT SCENARIO

In Sec. IV A we explicitly calculate the two-loop renormalizations of H and K_t. We show that logarithmic terms suppress the FP discussed in Secs. II and III. We then show that a large scaling region exists (at least near $d=2$) even though the FP is suppressed. We then give the effective exponents describing the scaling region.

A. Two-loop calculation of the H and K_t renormalization

We first calculate the H renormalization. It is obtained by considering the propagator $P^{(2)}_0$ at $k=0$. The calculation is simplified considerably if the non-Gaussian or nonlinear terms in Eq. (3.3) are effectively,

$$H_{\text{NL}} = H^{(4)}_0 + H^{(4)}_{I,\text{eff}} \ . \tag{4.1}$$

Equation (4.1) is valid as long as all relevant contributions arise from maximally contracted diagonal q fields in Eq. (3.4a). An exceptional diagram (cf. Fig. 3) where this is not the case will be discussed later.

The theory defined by Eq. (4.1) is simply a quartic field theory. We denote the vertex $H^{(4)}_0$ by a solid point as shown in Fig. 4(a), and the vertex $H^{(4)}_{I,\text{eff}}$ by an open square as shown in Fig. 4(b). In Fig. 4(b) we also show the connection with the original field theory where a small open circle indicates an "interacting" three- or four-point vertex.

In Fig. 5 we show the two-loop skeleton diagram that contributes to $P^{(2)}_0$. In Fig. 5(a), we also show the corresponding diagrams in the original theory. We find that the skeletons in Fig. 5(b) do *not* contribute relevant renormalizations to $\Gamma^{(2)}_0$. Denoting the contributions of the diagrams in Fig. 5(a) to $\Gamma^{(2)}_0$ by $\Gamma^{(2)}_{0,(5a)}$, we obtain

$$\Gamma^{(2)}_{0,(5a)} = \frac{3K_t^2}{4} G^3 \frac{(2\pi T)^2}{\omega_m} \sum_{n_1=1}^{m} \sum_{n_2=1}^{\infty} (\omega_m - \omega_{n_1}) \int_{\mathbf{p}_1\mathbf{p}_2} [1 - GK_t \omega_{n_1} D^t_{n_1}(p_1)]^2 D_{m-n_1}(\mathbf{p}_1) D_{n_2}(\mathbf{p}_2) D_{n_2+n_1}(\mathbf{p}_1+\mathbf{p}_2) \ . \tag{4.2a}$$

Dimensional regularization gives

$$\Gamma^{(2)}_{0,(5a)} \simeq H\omega_m \frac{3}{16\epsilon^2} \left[\frac{K_t}{H} \right]^2 \bar{G}^2 [1 + \epsilon L_t + \epsilon \ln(GH\omega_m) - 3\epsilon/2] + O(\epsilon^0) \ , \tag{4.2b}$$

with L_t from Eq. (2.16b). As mentioned earlier, we see here that the limit $K_t \to \infty$ cannot be taken inside the integrals because the n_1 sum in Eq. (4.2a) is bound by m. It is in this way that skeleton diagrams contribute terms of order $(K_t)^2$ even though $H_{\rm NL}$ is formally of order $(K_t)^0$.

Note the characteristic logarithmic term in Eq. (4.2b) (and following). In Sec. IV B we will show that terms like this eventually suppress the FP discussed in Sec. II. Physically these terms arise because the time or frequency scale associated with spin diffusion (D^t) is different from the time scale for D. Technically, they arise because finite-frequency sums do not allow the interchange of the $K_t \to \infty$ limit and frequency summation.

All remaining contributions to $P_0^{(2)}(k,m)$ are propagator renormalizations in the one-loop diagrams shown in Fig. 6. Note that the triplet propagator in Fig. 6(c) has already been renormalized by the last diagram in Fig. 5(a). To perform the remaining propagator renormalization, we denote the one-loop contribution to $\Gamma_0^{(2)}$ by $\Gamma_{0,1}^{(2)}$, and find its leading (for $K_t \to \infty$) contribution from Eq. (2.17b):

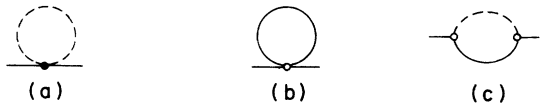

FIG. 6. One-loop diagrams for $\Gamma_0^{(2)}$.

$$\Gamma_{0,1}^{(2)}(k=0,m)=\frac{3GK_t}{4}\frac{(2\pi T)}{\omega_m}\sum_{n=1}^{m}(\omega_m-\omega_n)\int_{\rm p}D_n^t(\mathbf{p})-\frac{3GK_t}{4}\frac{2\pi T}{\omega_m}\sum_{n=1}^{m}\omega_n\int_{\rm p}D_n(\mathbf{p})[GK_t\omega_{m-n}D_{m-n}^t(\mathbf{p})-1]\ . \tag{4.3a}$$

Here the first term comes from the noninteracting nonlinearity $H_0^{(4)}$ in Eq. (3.3), while the second term is due to $H^{(3)}$ and $H_I^{(4)}$. To renormalize the propagators in Eq. (4.3a), we use $\Gamma_{0,1}^{(2)}$ itself and the corresponding one-loop contribution to $\Gamma_t^{(2)}$. The latter we denote by $\Gamma_{t,1}^{(2)}$, and near the proposed FP we find from Eq. (2.17f)

$$\Gamma_{t,1}^{(2)}(k,m)=\omega_m G^2K_t^2 2\pi T\int_{\rm p}\left[\sum_{n=1}^{\infty}D_n(\mathbf{p})D_{n+m}(\mathbf{k}+\mathbf{p})-\frac{1}{4}\left[\sum_{n=1}^{m-1}+\sum_{n=m}^{\infty}\frac{\omega_m}{\omega_n}\right]D_n^s(\mathbf{p})D_{n+m}(\mathbf{k}+\mathbf{p})\right]\ . \tag{4.3b}$$

The renormalization of the second term in Eq. (4.3a) does not contribute to leading order. For renormalizing the first term, it is important to realize that the factor of K_t is *not* a vertex, but rather was generated from a triplet propagator by the mechanism discussed in point (1) in Sec. III A. Therefore, this factor of K_t must be renormalized. Moreover, its renormalization is momentum and frequency dependent, and must be considered under the integrals. Denoting these two-loop contributions to $\Gamma_0^{(2)}$ by (6) we obtain

$$\Gamma_{0,(6)}^{(2)}=\Gamma_{0,(5a)}^{(2)}+O(\epsilon^0)\ . \tag{4.4}$$

This somewhat surprising result can be confirmed by considering the integrals themselves. Since we are only interested in UV-divergent contributions to $\Gamma_0^{(2)}$, we can neglect the second term in square brackets in Eq. (4.3b) as well as the frequency dependence of the first term. If we use the remaining expression for $\Gamma_{t,1}^{(2)}(k,0)$ in Eq. (4.3a), the integrals can be rearranged to give an expression identical with Eq. (4.2a) (apart from terms which vanish near the FP). Combining Eqs. (4.2b), (4.4), and (2.17b), the final result for $\Gamma_0^{(2)}$ to two-loop order near the proposed FP is

$$\Gamma_0^{(2)}(k,m)=\frac{k^2}{G}+H\omega_m-H\omega_m\frac{3\bar{G}}{4\epsilon}\left[\frac{K_t}{H}\right]+H\omega_m\frac{3}{8\epsilon^2}\left[\frac{K_t}{H}\right]^2\bar{G}^2[1+\epsilon L_t+\epsilon\ln(GH\omega_m)-3\epsilon/2]+O(\epsilon^0,G^3)\ . \tag{4.5}$$

Note that the diagrams associated with the renormalization of the triplet propagator in Fig. 6(a) are given in Fig. 3 and they are not in the theory defined by Eq. (4.1). This is the exceptional case mentioned earlier in this subsection. Following the proof of the first theorem in Sec. III A, it is clear that this diagrammatic "accident" can only happen with insertion diagrams. For skeleton diagrams, power counting works and the proofs in Sec. III A hold. Therefore, we can safely use Eq. (4) to generate all skeleton diagrams and then use lower-order results to evaluate all insertion diagrams.

The K_t renormalization can be computed by considering $P_t^{(2)}$. In fact, using arguments very similar to those that led to Eq. (3.6b), the K_t renormalization can be related to a four-point function to be calculated with the same

effective Hamiltonian as in Eqs. (3.6b) and (4.1). to see this, we follow Sec. III B and we write

$$P_t^{(2)}(k,m)=\langle \tilde{q}_m^{\alpha\alpha}(\mathbf{k})\tilde{q}_m^{\alpha\alpha}(\mathbf{k})^*\rangle_c^H$$
$$=\left\langle \tilde{q}_m^{\alpha\alpha}(\mathbf{k})\tilde{q}_m^{\alpha\alpha}(\mathbf{k})^* \sum_{n=0}^{\infty}\frac{(H^{(3)})^{2n}}{(2n)!}\right\rangle_c^{H^{(2)}+H^{(4)}} . \quad (4.6)$$

Now, the difference with Eq. (3.6a) is that the diagonal q fields in $(H^{(3)})^{2n}$ *can* be contracted with the external or end-point q fields. Again, using simple combinatorial arguments, the leading (as $K_t\to\infty$) order result for $\Gamma_t^{(2)}(k,m)$ is

$$\Gamma_t^{(2)}(k,m)=(k^2/G)+(H+K_t)\omega_m+\Delta_1+\Delta_2 , \quad (4.7)$$

where

$$\Delta_1=-K_t^2G^2\omega_m\pi T\sum_{\{\alpha_1,i_1,j,n\}}\int_{\mathbf{p}_1\mathbf{p}_1'}(-1)^{j_1+j_2}\langle q_{nn_1}^{\alpha\alpha_1,j_1i_1}(\mathbf{p}_1)q_{n+m,n_1}^{\alpha\alpha_1,j_2i_1}(\mathbf{p}_1+\mathbf{k})^*q_{n'n_1'}^{\alpha\alpha_1'j_2i_1'}(\mathbf{p}_1')q_{n'-m,n_1'}^{\alpha\alpha_1',j_1i_1'}(\mathbf{p}_1'-\mathbf{k})^*\rangle_c^{H^{(2)}+H_{\rm NL}} \quad (4.8a)$$

and

$$\Delta_2=K_t^2G^2\omega_m 2\pi T\sum_{\{\alpha_1,i_1,j,n\}}\int_{\mathbf{p}_1,\mathbf{p}_1'}(-1)^{j_1+j_2}\langle q_{nn_1}^{\alpha\alpha_1,j_1i_1}(\mathbf{p}_1)q_{n+m,n_1}^{\alpha\alpha_1,j_2i_1}(\mathbf{p}_1+\mathbf{k})^*q_{n_1'n'}^{\alpha\alpha_1',i_1'j_2}(\mathbf{p}_1')^*q_{n_1',n'-m}^{\alpha\alpha_1',i_1'j_1}(\mathbf{k}-\mathbf{p}_1')\rangle_c^{H^{(2)}+H_{\rm NL}} . \quad (4.8b)$$

To make a connection with the results of Sec. II we evaluate Eqs. (4.8) in the Gaussian approximation which corresponds to the one-loop theory for $\Gamma_t^{(2)}$. To leading order as $K_t\to\infty$, $\Delta_1+\Delta_2$ gives Eq. (4.3b). Diagrammatically, we show this one-loop contribution in Fig. 7(a).

At two-loop order we again have two-types of contributions: (i) propagator renormalizations in the one-loop result and (ii) new skeleton diagrams. The propagator renormalization class can be computed by using Eq. (4.3a) in Eq. (4.3b). Denoting this contribution by $\Gamma_{t,2a}^{(2)}$, we obtain

$$\Gamma_{t,2a}^{(2)}(k,m)=-K_t\bar{G}^2\omega_m\frac{3}{8\epsilon^2}\left[\frac{K_t}{H}\right]^2$$
$$\times\left[1+\frac{\epsilon}{2}[L_t-L_s\ln 2+2\ln(GH\omega_m)]\right.$$
$$\left.+\frac{\epsilon}{4}[-9+(\pi^2/12)-2\ln 2+(\ln 2)^2]\right] . \quad (4.9a)$$

Note that Δ_1 and Δ_2 in Eqs. (4.7) and (4.8) have a prefactor of ω_m. This implies that none of the internal frequency sums in Eq. (4.8) can be finite sums bounded by the external frequency ω_m. Therefore, the mechanism by which skeleton diagrams contributed to $\Gamma_0^{(2)}$ [cf. the remark following Eq. (4.2b)] is not effective here. However, there is another mechanism. If the second term in Eq.

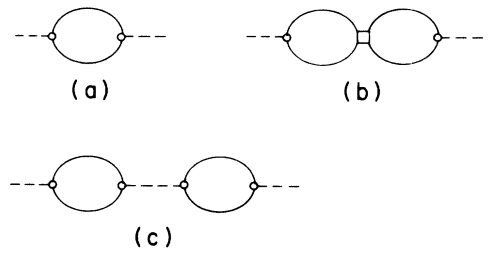

FIG. 7. (a) One-loop diagram for $\Gamma_t^{(2)}$. (b) Two-loop skeleton diagram for $\Gamma_t^{(2)}$. (c) One-particle reducible diagram arising from the skeleton diagram in the effective-field theory.

(3.7b) is at the external wave number and frequency (here k,ω_m), then it should be interpreted as a one-particle reducible diagram and it does not contribute to $\Gamma_t^{(2)}$. For this case the two terms in Eq. (3.7b) do *not* cancel as $K_t \to \infty$. In terms of diagrams, this is shown in Figs. 7(b) and 7(c). $K_t \to \infty$ is equivalent to replacing a dashed line by a point. In this case the diagrams in Fig. 7(b) are of equal magnitude but of opposite signs and they cancel each other. However, Fig. 7(c) [which is contained in Fig. 7(b)] does not contribute to $\Gamma_t^{(2)}$ because it is a reducible diagram. Denoting the remaining contribution to $\Gamma_t^{(2)}$ by $\Gamma_{t,2b}^{(2)}$, we obtain

$$\Gamma_{t,2b}^{(2)}(k,m)=K_t\bar{G}^2\frac{\omega_m}{\epsilon^2}\left[\frac{K_t}{H}\right]^2\{1+\epsilon[\ln(GH\omega_m)-\tfrac{1}{2}L_s\ln 2]+\epsilon[-1+\pi^2/48+\tfrac{1}{4}(\ln 2)^2]\}\ . \tag{4.10}$$

Combining Eqs. (4.9), (4.10), and (2.17), the final result for $\Gamma_t^{(2)}$ to two-loop order near the proposed FP is

$$\Gamma_t^{(2)}(k,m)=\frac{k^2}{G}+(H+K_t)\omega_m-K_t\omega_m\frac{G}{\epsilon}\left[\frac{K_t}{H}\right]+K_t\omega_m\frac{5\bar{G}^2}{8\epsilon^2}\left[\frac{K_t}{H}\right]^2\{1+\epsilon[-\tfrac{3}{10}L_t-\tfrac{1}{2}L_s\ln 2+\ln(GH\omega_m)-\tfrac{1}{4}+\pi^2/48+\tfrac{3}{10}\ln 2+\tfrac{1}{4}(\ln 2)^2]\}+O(\epsilon^0,\bar{G}^3)\ . \tag{4.11}$$

The two-loop term of $O(1/\epsilon^2)$ was determined before[16] as a check of renormalizability.

We conclude this subsection by reviewing the four mechanisms by which the conclusion that $H_{\rm NL}$ is of order $(K_t)^0$ can be avoided. We argue that none of these mechanisms invalidate the proof of $s=0$ in Sec. III B.

(i) Finite-frequency sums with an upper limit of external frequency. This mechanism is argued to be irrelevant for the $s=0$ proof following Eq. (3.7).

(ii) The second term in Eq. (3.7b) can be at the external wave number and frequency. In this case [as explained following Eq. (4.9)] it should be interpreted as a one-particle reducible diagram and, consequently, the two terms in Eq. (3.7b) do not cancel. It is clear that this cannot happen in the disorder renormalization in $P_0^{(2)}$ because in this case all reducible diagrams involve only the propagator D.

(iii) The breakdown of Eq. (4.1) discussed following Eqs. (4.1) and (4.5). These diagrams are insertions. For the disorder renormalization there are no relevant skeleton diagrams because (i) and (ii) are not operative. Therefore, insertions are irrelevant for g.

(iv) Insertion diagrams with finite-frequency sums with an upper limit on internal frequency. Again, insertions are irrelevant for the disorder renormalization since no skeleton diagrams exist.

B. Two-loop RG flow equations and scaling

We now use the renormalization procedure described in Sec. II B to determine the RG flow equations to two-loop order. From Eqs. (2.24b) and (2.24d) together with Eqs. (4.5) and (4.11) we find the renormalization constants to leading order for $K^t \to \infty$:

$$Z_H=1+\frac{3}{4\epsilon}y+\frac{3}{8\epsilon^2}y^2(1+\epsilon)+O(g^3)\ , \tag{4.12a}$$

$$Z_t=1+\frac{1}{\epsilon}y+\frac{5}{8\epsilon^2}y^2[1+\epsilon(\tfrac{3}{10}l_t-\tfrac{3}{20})]+O(g^2)\ . \tag{4.12b}$$

This yields the following flow equations:

$$b\frac{dh}{db}=h\tfrac{3}{4}y+h\tfrac{3}{4}y^2+O(g^3)\ , \tag{4.13a}$$

$$b\frac{d\gamma_t}{db}=\gamma_t\tfrac{1}{4}y+\gamma_t\tfrac{3}{8}y^2l_t-\gamma_t\tfrac{15}{16}y^2+O(g^3)\ , \tag{4.13b}$$

$$b\frac{dy}{db}=-\epsilon y+\tfrac{1}{4}y^2+\tfrac{3}{8}y^3l_t-\tfrac{15}{16}y^3+O(g^4)\ . \tag{4.13c}$$

Comparing with the criteria given in Sec. III A, we see that Eq. (4.13a) is consistent with the FP scenario, but Eqs. (4.13b) and (4.13c) are not. The reason is the logarithmic term at two-loop order, the mathematical origin of which has been extensively discussed in Sec. IV A. We note that the power-counting arguments used in Sec. III are insensitive to these terms, so that they can only be found by an explicit calculation. We also note that the terms proportional to l_s which appear in $\Gamma_t^{(2)}$, cf. Eqs. (2.25d) and (4.11), are absent from the flow equations due to nontrivial cancellations.

For a discussion of Eqs. (4.13), let us first ignore the two-loop terms. Then Eq. (4.13c) shows a trivial fixed point at $y=0$, and a nontrivial one at $y=y^*=4\epsilon+O(\epsilon^2)$. The flow in the $g-\gamma_t$ plane is shown schematically in Fig. 8(a). For subcritical values of $y^0=y(b^0)<y^*$, the RG flow approaches the axis $g=0$ representing the clean Fermi liquid. For $y^0=y^*$, the flow approaches the stable FP at $g=0$, $\gamma_t=\infty$. For larger values of y^0, γ_t reaches infinity at a finite-length scale. We note that this does not

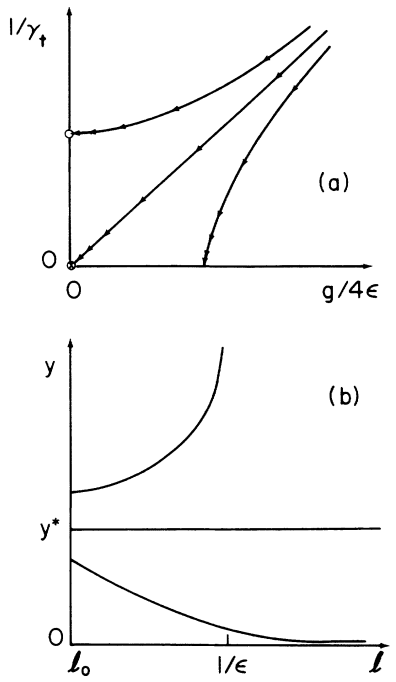

FIG. 8. (a) Schematic flow diagram for the FP scenario. The circle denotes a Fermi liquid FP. The crossed circle denotes the nontrivial FP $y^*=4\epsilon$ with y as defined before Eq. (2.22a). (b) Schematic plot of y as a function of $l=\ln b$ for three different initial values y^0 corresponding to the three trajectories in (a).

signalize a deficiency of the theory, but is simply due to the fact that in this regime Eq. (4.13c) is not an adequate representation of the RG β function. The same phenomenon is found in the noninteracting localization problem, where an approximate expression for the β function on the insulating side is known.[17] In Fig. 8(b) we schematically show y as a function of the scale $l=\ln b$. For $y^0<y^*$, y decreases on a scale $l\sim 1/\epsilon$, and approaches zero for $l\to\infty$. For $y^0>y^*$, y diverges at a finite scale $l\sim 1/\epsilon$. Ignoring the two-loop terms, we thus have a consistent interpretation of our results in terms of a transition where the spin-diffusion constant vanishes. The correlation length exponent is found by linearizing Eq. (2.22d) about the FP $y^*=4\epsilon$. This yields

$$\nu=\frac{1}{\epsilon}+O(\epsilon^0)\ . \tag{4.14a}$$

We denote the dimensionless distance from the FP by $t\equiv|y-y^*|$, and at zero temperature we choose $b=t^{-\nu}$. Then h diverges as $h\sim t^{-\kappa}$ (this defines the exponent κ), with

$$\kappa=3+O(\epsilon)\ . \tag{4.14b}$$

The exponent κ determines the divergence of the specific-heat coefficient $\gamma=\lim_{T\to 0}C/T$, where C is the specific heat. γ is given[18] by $\gamma\sim\gamma_0(2/\pi N_F)h\sim t^{-\kappa}$, where γ_0 is the free-electron result. Furthermore, the static spin susceptibility is given by[19]

$$\chi_s\sim\chi_s^0(2/\pi N_F)(h+k_t)=(2/\pi)h(1+y/g)\sim t^{-\gamma}\ .$$

Here χ_s^0 is the Pauli susceptibility, and

$$\gamma=\kappa+\nu\theta=4+O(\epsilon)\ . \tag{4.14c}$$

We also determine the behavior of the spin-diffusion coefficient in the scaling region. The time scale in the triplet channel is determined by the scaling behavior of k_t, cf. Eq. (2.25d). As in Eq. (2.23), we must remember that g is dangerously irrelevant. The dynamical spin-diffusion coefficient obeys the scaling law

$$D_s(g,t,\omega)=b^{-\epsilon-\gamma/\nu}D_s(gb^{-\theta},tb^{1/\nu},\omega b^{2+\kappa/\nu})\ . \tag{4.15a}$$

In the static limit, and using $D_s(g\to 0)\sim 1/g$, we find

$$D_s(t)\sim t^{\gamma}\ , \tag{4.15b}$$

where γ has been given in Eq. (4.14c). Alternatively, Eq. (4.15b) follows directly from Eq. (2.23b). We note that due to the identity $\theta=\epsilon$, the exponents describing the vanishing of D_s, and the divergence of χ_s, are the same. At the FP we find

$$D_s(\omega)\sim\omega^{\gamma/(2\nu+\kappa)}\ . \tag{4.15c}$$

We note that the last result is of somewhat formal nature. In view of the different time scales we encountered, the physical meaning of the dynamical exponent is not quite clear.

In contrast to these nonzero exponents which characterize the spin system, the exponents for the conductivity and the DOS both vanish, as has been shown in Sec. III. We reemphasize that at this point we cannot tell whether a vanishing exponent means noncritical or discontinuous behavior.

In order to determine the scaling behavior at nonzero temperatures, we need a relation between T and b. Let us denote the scaling dimension of T by $[T]$. Dimensional analysis of the term proportional to H in Eq. (2.4) shows $[T]=2+\kappa/\nu$, where κ is given by Eq. (4.14b).[20] The temperature dependence at the FP of the quantities discussed earlier can therefore be obtained by the replacement

$$t\to T^{1/(2\nu+\kappa)}\ . \tag{4.16}$$

Let us now take the two-loop terms in Eqs. (4.13) into account. This changes the picture qualitatively. For $g\to 0$, l_t grows beyond limits, and the FP is destroyed. Furthermore, even for $y^0<y^*$ the trajectories do not approach the trivial Fermi-liquid fixed points anymore, but rather γ_t diverges at a finite (f) length scale $l_f\sim 1/\epsilon^{3/2}$. The trajectories in the $1/\gamma_t-g$ plane are shown schematically in Fig. 9(a). The behavior of $y(l)$ is shown schematically in Fig. 9(b). Note that for $y^0<y^*$, y first decreases on a scale $l\sim 1/\epsilon$ before it turns around and diverges at the larger scale $l_f\sim 1/\epsilon^{3/2}$.

It is evident from this discussion that at least for small ϵ the different length scales are well separated, and the flow follows the trajectories of the FP scenario a long way before it is driven away by the logarithmic terms at a length scale l_f. The corresponding finite-temperature

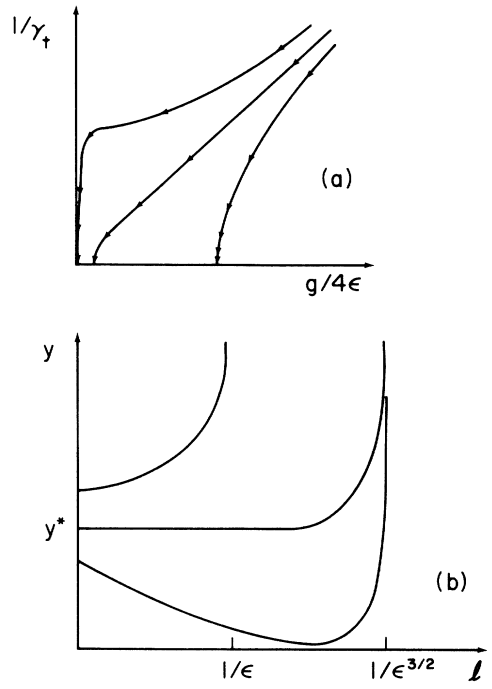

FIG. 9. (a) Schematic flow diagram for the suppressed nontrivial FP. (b) Corresponding plot of $y(l)$.

scale, where deviations from scaling will become manifest, is

$$T_f = T_0 \exp[-c\epsilon^{-3/2} + O(\epsilon^{-1/2})] , \tag{4.17}$$

where c is a numerical factor of $O(1)$ and T_0 is a temperature corresponding to the microscopic length scale b_0. At least close to $d=2$, we are thus guaranteed the existence of a scaling regime, where the system shows incipient spin localization. In this regime the observables like D_s, γ, and χ_s scale with the exponents given above. We have thus identified the exponents of the FP scenario as "effective exponents" which describe the system in a scaling region close to the suppressed spin localization FP. At asymptotically large length scales, $l > l_f$, or asymptotically low temperatures, $T < T_f$, scaling ceases to be valid. Rather than undergoing a phase transition, the system crosses over to some other behavior. The nature of this asymptotic regime cannot be explored with our present technique.

We close this section with two remarks. (i) In $d=3$ it is *a priori* unclear if the time scales are still separated and if there is any scaling region. However, there is some experimental evidence for a near instability in the spin transport of the kind discussed above even in three-dimensional systems. We will discuss this in Sec. V. (ii) Our result that the FP is suppressed lifts the ambiguity in the interpretation of the vanishing exponents for the conductivity and the DOS. Since there is no phase transition, a discontinuity can be ruled out. The only remaining interpretation is that the conductivity and the DOS are noncritical throughout the scaling region around the near instability in the spin system.

V. DISCUSSION

A. Interpretation of results

Let us summarize our results. The one-loop analysis[3–8,18,19] of the model considered here suggests the possibility of a phase transition. While initially the corresponding FP was thought to describe a MIT,[7] it has been suggested that it could instead be related to an instability in the spin system.[21] Our results show explicitly that the former interpretation is incorrect. We have used power counting to show that necessary conditions for the existence of this FP are fulfilled to all orders in a loop expansion. Indeed this proves the existence of the FP apart from possible logarithmic terms which cannot be distinguished from constants by means of power counting. We have then shown by an explicit two-loop calculation that logarithmic terms do appear, starting at two-loop order, which suppress the FP. We note that the main argument for a MIT in Ref. 7 was the fact that the quasiparticles were found to be localized. The suppression of the FP eliminates the basis for this interpretation. Since there is no phase transition, no degrees of freedom are actually localized. We therefore believe that the only possible interpretation of our result $s=0$ is that of an uncritical conductivity. The physical picture which emerges is as follows. With increasing disorder at zero temperature, spin diffusion in the Fermi liquid slows down. As the (bare) disorder approaches a critical value, which is proportional to the inverse (bare) interaction strength, the system enters a critical region which shows all signs of an incipient spin-localization transition. The spin-diffusion constant scales towards zero, and the magnetic susceptibility and the specific-heat coefficient scale towards infinity. The corresponding exponents have been calculated in Sec. IV B. Throughout this scaling region, the charge-diffusion constant or the electrical conductivity and the density of states at the Fermi level are decoupled from the spin dynamics and show no critical behavior. With further increasing disorder, scaling ceases to be valid before the spin system reaches an actual instability. Instead of entering a spin-insulator phase, the system crosses over to some as yet unexplored regime characterized by slow-spin transport.

In physical terms we interpret our results as follows. The correlations in the repulsively interacting Fermi system tend to localize the electronic degrees of freedom. This is why the critical disorder is proportional to the inverse interaction strength. This localization tendency is most pronounced for the spin, whose diffusion coefficient decreases monotonically. The resulting slow-spin fluctuations in turn have a tendency to increase the charge-diffusion coefficient.[22] For the latter, localizing and delocalizing tendencies keep a balance, so that the charge transport is not critically affected by the slowing down of the spin dynamics. If we ignore the suppression of the spin-localization transition for a moment, this means that the system enters a metallic phase which is a spin insula-

tor. This means that the strong correlations have created an environment with local preferred spin directions. Charge and, therefore, mass are still mobile, and the electrons adjust their spin to the local environment as they move around. One might call this system an itinerant random magnet. In reality, the spins do not quite undergo a phase transition. However, the correlation length becomes exponentially large, and so one still expects domains of preferred spin directions which fluctuate only very slowly. This picture is consistent with earlier implicit suggestions,[23] and bears a remarkable resemblance to the concept of spontaneous formation of local magnetic moments discussed recently by Milovanovich *et al.*[24] The model under consideration, Eq. (2.2a) with a short-range interaction potential, is a generalization of a Hubbard model with disorder. One would therefore expect that at least some properties even of the effective model, Eq. (2.4), are very similar to those of a Hubbard model. We note, however, that in Ref. 24 off-diagonal disorder seems to play an important role. In addition, in the present model the Cooper channel has been omitted, whose inclusion could introduce a stronger tendency towards localization. The relation, if any, between these two approaches is therefore not quite clear. With further increasing disorder, one expects the system to undergo a MIT. We expect the detailed properties of this transition to be severely influenced by the slow-spin dynamics. It is therefore not clear that this transition will fall into one of the known universality classes.[4,6] In order to study the MIT, one has to consider the coupling between charge and spin degrees of freedom (since k_t does not actually diverge, this coupling is nonzero). It is conceivable to do this by keeping next-leading terms in the expansion for large k_t, the leading terms of which we have used in this paper. However, our present RG technique does not permit us to study the far side of the (suppressed) FP. A description of the region of slow-spin transport, and eventually of the MIT, will therefore require a technically different approach.

Before we discuss the experimental situation, we mention those points which might preclude a direct comparison between our theory and experiment. (i) All of our conclusions are strictly valid only in $d=2+\epsilon$ dimensions. Little is known about the convergence properties of the ϵ expansion (presumably they are poor), and any application to $d=3$ is somewhat speculative. (ii) We have used a short-ranged model interaction. (iii) We have neglected the Cooper channel. These two approximations have been discussed in Sec. II A.

B. Discussion of experiments

Most experiments performed so far have concentrated on the MIT.[25] In this context the value of the conductivity exponent s has given rise to much discussion. While in most classes of materials $s\cong 1$ is observed, uncompensated multivalley semiconductors show $s<1$. The most well-known case is Si:P with $s\cong 0.5$.[26] Such small values of s pose a formidable theoretical problem. Wegner scaling,[14] $s=\nu\epsilon$, together with the rigorous bound[27] $\nu\geq 2/d$, implies $s\geq\frac{2}{3}$ in $d=3$ There is one known mechanism to avoid Wegner scaling for the conductivity. It is related to a dangerously irrelevant variable[7] and has been discussed in this paper [cf. Eq. (2.24c)]. It was a promising suggestion[28] that uncompensated semiconductors might be in a universality class with $\theta\neq 0$. However, in the light of the present results this seems very unlikely. Since the system avoids the FP with $\theta\neq 0$, it is hard to imagine that the scenario could be successfully repeated at *larger* disorder. The experimental findings on this point are thus at odds with very well established theoretical results. It is of course possible that some exotic property of the regime of slow-spin transport will lead to yet another mechanism for violating Wegner scaling, but at this point this is pure speculation.

Let us finally discuss some recent experiments which provide some information about spin transport in the metallic phase and thus relate more directly to our calculation. Ikehata and Kobayashi[29] measured the magnetic susceptibility χ in Si:P. They find a sharp increase of χ at low temperatures, even deep inside the metallic phase. Indeed the anomaly seems to be more pronounced 50% away from the MIT than very close to it, and no qualitative change of the behavior was observed while crossing the MIT. These results are consistent with a near instability in the spin system well in the metallic phase. Alloul and Dellouve[30] studied ^{31}P NMR spectra in Si:P, and concluded that there is a fraction of spins which are localized even in the metallic phase. This fraction monotonically increased through the MIT. In interpreting this experiment one should keep in mind that it may be very hard to experimentally distinguish between our regime of slow-spin transport and an actual spin insulator. Finally, Paalanen *et al.*[31] measured the specific heat of Si:P, and compared the results with earlier data[32] of the spin susceptibility for the same samples. They find that both χ_s and γ, as well as the Wilson ratio $w=(\chi_s/\chi_s^0)/(\gamma/\gamma_0)$, increase at low temperature even in the metallic phase. w eventually saturates at very low temperatures. Thereby the saturation temperature seems to increase with decreasing donor density.

It has been argued[33,34,24] that these experimental results cannot be understood on the basis of a theory which concentrates on diffusive modes, but rather provide evidence for the importance of electronic states deep below the Fermi surface. We are not convinced that this is necessarily the case. As we have discussed in Sec. V A, diffusion physics is capable of spontaneously generating a spin state which has much in common with local moments. We also stress that NMR is a local probe, so it is not surprising to find a finite fraction of spins which appear to be localized. If there was a local probe of charge transport, one would see a finite fraction of electrons which appear to be localized on either side of the MIT. The number of 'localized' electrons would depend on the length scale one is looking at.

Let us go back to the measurement of the Wilson ratio, and discuss in detail what we would expect to see based on our theoretical results. Combining Eqs. (4.14b) and (4.14c), we get at zero temperature

$$w\sim t^{-\nu\theta}\,, \tag{5.1}$$

where $\theta=\epsilon$ we know exactly from Sec. III B. For ν we can use again the bound[27] $\nu \geq 2/d$. Therefore we find that in three dimensions at zero temperature, w increases with an exponent which exceeds $\frac{2}{3}$ as we cross the scaling region coming from the spin metallic side. Scaling will stop, and w will show some different behavior once a separation

$$t_f \sim b_f^{\nu} \sim \exp[\text{const}\epsilon^{-3/2}+O(\epsilon^{-3/2})]$$

from the suppressed FP has been reached. For fixed $t \ll 1$, w will increase with decreasing temperature as

$$w \sim T^{-\mu} , \tag{5.2a}$$

$$\mu=\frac{\theta\nu}{2\nu+\kappa}=\frac{\epsilon/2}{1+3\epsilon/2+O(\epsilon^2)} , \tag{5.2b}$$

according to Eq. (4.16). At $t=0$, scaling will cease to be valid below a temperature $T_f \sim t_f^{d\nu+\kappa}$. At $t=0$ with decreasing temperature, w will cross over from the behavior shown in Eq. (5.2) to the constant value given in Eq. (5.1) above the suppressed transition and to some unknown behavior below it. The crossover temperature obeys $T_{\rm cr}^{-\theta/(d+\kappa/\nu)} \sim t^{-\nu\theta}$, or

$$T_{\rm cr} \sim t^{2\nu+\kappa}=t^{(2/\epsilon)[1+O(\epsilon)]} . \tag{5.3}$$

This behavior is summarized schematically in Fig. 10. In an experiment like the one in Ref. 31, one scans this diagram for a given donor concentration along a vertical line as indicated in Fig. 10. We thus expect w to increase with exponent μ, and then to saturate at a temperature $T_{\rm cr}$. The results of Ref. 31 are consistent with this expectation with an exponent $\mu \simeq \frac{1}{3}$. The value of $T_{\rm cr}$ in Ref. 31 seems to increase with decreasing donor concentration. This is consistent with our interpretation if we assume that all three samples studied were on the "spin-insulating" side of the suppressed spin-localization transition. Since the highest donor concentration was only 25% above the MIT, this is entirely possible. It is also consistent with our scenario that no qualitative change in the behavior of w was observed in going from the metallic to the insulating phase.

We find this qualitative agreement very encouraging, and suggest the following experiment to further test the theory. Systematic measurements of w in the *metallic* phase should yield a "critical" donor concentration n^*. For $n > n^*$, the saturation temperature $T_{\rm cr}$ should decrease with decreasing n; for $n < n^*$ it should increase.

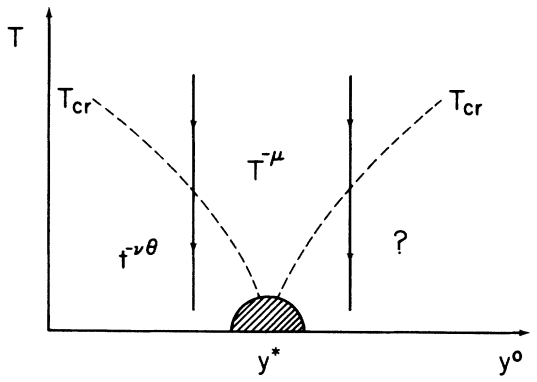

FIG. 10. Schematic plot of the scaling region predicted for the Wilson ratio. In the shaded region scaling breaks down. The behavior in the region denoted by "?" is unknown. The vertical lines show the path followed in an experiment when the temperature is lowered at fixed impurity concentration.

Both $w(T)$ and $T_{\rm cr}(t=|n/n^*-1|)$ should scale with exponents given by Eqs. (5.2) and (5.3), respectively. Since θ is known exactly, this will be sufficient to determine ν and κ. Furthermore, the saturation value $w(T \ll T_{\rm cr})$ for $n > n^*$ should scale according to Eq. (5.1). Since ν is known already, this will be a stringent test for our scaling scenario.

ACKNOWLEDGMENTS

Work at the University of Maryland was supported by the National Science Foundation under Grant No. DMR-86-07605 and by the Presidential Young Investigator Program. Work at the University of Oregon was supported in part by the National Science Foundation under Grant No. DMR-88-19302. Acknowledgment is made to the donors of the Petroleum Research Fund administered by the American Chemical Society for partial support of this research. Partial support by the Materials Science Institute at the University of Oregon is also gratefully acknowledged. D.B. would also like to thank the Center for Superconductivity Research at the University of Maryland for their generous hospitality.

APPENDIX

Here we list the frequency sums in terms of which the one-loop result was expressed in Eqs. (2.17b), (2.17d), and (2.17f):

$$I_1^{s,t}(\mathbf{p})=\frac{1}{4m}\sum_{l=1}^{m-1}\Delta D_l^{s,t}(\mathbf{p})+\tfrac{1}{4}\sum_{l=m}^{\infty}\frac{1}{l}\Delta D_l^{s,t}(\mathbf{p}) , \tag{A1}$$

$$I_2^{s,t}(\mathbf{p})=\frac{1}{4m}\sum_{l=1}^{m-1}\left[\frac{l}{m}-1\right][\Delta D_l^{s,t}(\mathbf{p})-G\omega_l K_{s,t} D_l^{s,t}(\mathbf{p}) D_{m-l}(\mathbf{k}-\mathbf{p})]$$
$$+\frac{1}{4m}\sum_{l=1}^{\infty}[\Delta D_l^{s,t}(\mathbf{p})+G\omega_l K_{s,t} D_l^{s,t}(\mathbf{p}) D_{l+m}(\mathbf{p}+\mathbf{k})] . \tag{A2}$$

$$J_1(\mathbf{p})=\frac{1}{4m}\sum_{l=1}^{m-1}\left[\left[1-\frac{l}{m}\right]D_{l+m}(\mathbf{p})+\frac{l}{m}D_l(\mathbf{p})\right], \tag{A3}$$

$$\tilde{I}_2^{s,t}(\mathbf{p})=\frac{1}{4m}\left[\sum_{l=1}^{m-1}\frac{l}{m}+\sum_{l=m}^{\infty}\right][\Delta D_l^{s,t}(\mathbf{p})+G\omega_l K_{s,t}D_l^{s,t}(\mathbf{p})D_{l+m}(\mathbf{p}+\mathbf{k})], \tag{A4}$$

$$\begin{aligned}J_2(\mathbf{p})=&\frac{G}{4}K_s\left[\sum_{l=1}^{m-1}\frac{l}{m}+\sum_{l=m}^{\infty}\right]\frac{m}{l}[\Delta D_l^s(\mathbf{p})D_{l+m}(\mathbf{p}+\mathbf{k})+3\Delta D_l^t(\mathbf{p})D_{l+m}(\mathbf{p}+\mathbf{k})]\\&+\frac{G}{2}\left[\sum_{l=1}^{m-1}\frac{l}{m}+\sum_{l-m}^{\infty}\right][K_sD_l^s(\mathbf{p})D_{l+m}(\mathbf{p}+\mathbf{k})+3K_tD_l^t(\mathbf{p})D_{l+m}(\mathbf{p}+\mathbf{k})],\end{aligned} \tag{A5}$$

$$\begin{aligned}J_3(\mathbf{p})=&-\left[\sum_{l=1}^{m-1}\frac{l^2}{m^2}+\sum_{l=m}^{\infty}\right]\frac{1}{l}\Delta D_l^t(\mathbf{p})-GK_t\sum_{l=1}^{\infty}D_l(\mathbf{p})D_{l+m}(\mathbf{p}+\mathbf{k})\\&+\frac{G}{4}K_t\left[\sum_{l=1}^{m-1}\left[3+2\frac{l}{m}-4\frac{l^2}{m^2}\right]+\sum_{l=m}^{\infty}\left[2-\frac{m}{l}\right]\right]D_l^t(\mathbf{p})D_{l+m}(\mathbf{p}+\mathbf{k})\\&+\frac{G}{2}K_s\left[\sum_{l=1}^{m-1}\frac{l}{m}+\sum_{l=m}^{\infty}\right]D_l^s(\mathbf{p})D_{l+m}(\mathbf{p}+\mathbf{k})+\frac{G}{4}K_t\left[\sum_{l=1}^{m-1}\frac{l}{m}+\sum_{l=m}^{\infty}\right]\frac{m}{l}D_l^s(\mathbf{p})D_{l+m}(\mathbf{p}+\mathbf{k}).\end{aligned} \tag{A6}$$

---

*Permanent address: Department of Physics and Materials Science Institute, University of Oregon, Eugene, Oregon 97403.

[1]F. Wegner, Z. Phys. B **35**, 207 (1979).

[2]A discussion of the nonlinear σ model and the field-theoretic techniques used in this paper can be found in D. J. Amit, *Field Theory, the Renormalization Group, and Critical Phenomena* (World Scientific, Singapore, 1984).

[3]A. M. Finkelshtein, Zh. Eksp. Teor. Fiz. **84**, 168 (1983) [Sov. Phys.–JETP **57**, 97 (1983)].

[4]A. M. Finkelshtein, Zh. Eksp. Teor. Fiz **86**, 367 (1984) [Sov. Phys.–JETP **59**, 212 (1984)]; Z. Phys. B **56**, 189 (1984).

[5]C. Castellani, C. Di Castro, G. Forgacs, and S. Sorella, Solid State Commun. **52**, 261 (1984).

[6]C. Castellani, C. Di Castro, P. A. Lee, and M. Ma, Phys. Rev. B **30**, 527 (1984).

[7]C. Castellani, G. Kotliar, and P. A. Lee, Phys. Rev. Lett. **59**, 323 (1987).

[8]D. Belitz and T. R. Kirkpatrick, Nucl. Phys. B **316**, 509 (1989).

[9]T. R. Kirkpatrick and D. Belitz, Phys. Rev. B **40**, 5227 (1989).

[10]D. Belitz and T. R. Kirkpatrick Phys. Rev. Lett. **63**, 1296 (1989).

[11]See, e.g., V. N. Popov, *Functional Integrals in Quantum Field Theory and Statistical Physics* (Reidel, Boston, 1983).

[12]See, for example, G. Grinstein in *Fundamental Problems in Statistical Physics VI* (North Holland, Amsterdam, 1985), p. 147.

[13]M. Grilli and S. Sorella, Nucl. Phys. B **295** [FS21], 422 (1988).

[14]F. Wegner, Z. Phys. B **25**, 327 (1976).

[15]C. De Dominicis and L. Peliti, Phys. Rev. B **18**, 353 (1978).

[16]C. Castellani, C. Di Castro, and S. Sorella, Phys. Rev. B **34**, 1349 (1986).

[17]D. Vollhardt and P. Wölfle, Phys. Rev. Lett. **48**, 699 (1982).

[18]C. Castellani and C. Di Castro, Phys. Rev. B **34**, 5935 (1986).

[19]This can be seen in the following way. For our time-reversal invariant system, the spin and charge mobilities (or conductivities) are identical. The Einstein relation for the spin transport therefore yields $D_s\chi_s=\sigma\sim 1/G$. With Eq. (2.23b) we find $\chi_s\sim(1/b^{\epsilon}g)b^{\epsilon}g(h+k_t)=h+k_t$. This agrees with the result obtained by C. Castellani, C. Di Castro, P. A. Lee, M. Ma, S. Sorella, and E. Tabet, Phys. Rev. B **33**, 6169 (1986).

[20]The fact that the "bare" dimension of T, as well as that of ω, Eq. (4.15a), is 2 rather than d is due to the fact that g is dangerously irrelevant and frequencies or temperatures always appear multiplied by g. See also Ref. 18.

[21]C. Di Castro, in *Anderson Localization,* edited by T. Ando and H. Fukuyama (Springer, New York, 1988), p. 96.

[22]R. Oppermann, Solid State Commun. **44**, 1297 (1982).

[23]A. M. Finkelshtein, Pis'ma Zh. Eksp. Teor. Fiz. **40**, 63 (1984) [JETP Lett. **40**, 796 (1984)].

[24]M. Milovanovich, S. Sachdev, and R. N. Bhatt, Phys. Rev. Lett. **63**, 82 (1989).

[25]Recent experimental results can be found, e.g., in the *Proceedings of the 31st Scottish University Summer School in Physics, St. Andrews, 1986,* edited by D. M. Finlayson (Edinburgh University, Edinburgh, 1987); *Anderson Localizations,* Ref. 21.

[26]T. F. Rosenbaum, K. Andres, G. A. Thomas, and R. N. Bhatt, Phys. Rev. Lett. **45**, 1723 (1980).

[27]J. Chayes, L. Chayes, D. S. Fisher, and T. Spencer, Phys. Rev. Lett. **57**, 2999 (1986).

[28]G. Kotliar, in *Anderson Localization,* Ref. 21, p. 107.

[29]S. Ikehata and S. Kobayashi, Solid State Commun. **56**, 607 (1985); S. Ikehata, in *Anderson Localization,* Ref. 21, p. 18.

[30]H. Alloul and P. Dellouve, Phys. Rev. Lett. **59**, 578 (1987).

[31]M. A. Paalanen, J. E. Graebner, R. N. Bhatt, and S. Sachdev, Phys. Rev. Lett. **61**, 597 (1988).

[32]M. A. Paalanen, S. Sachdev, R. N. Bhatt, and A. E. Ruckenstein, Phys. Rev. Lett. **57**, 2061 (1986).

[33]A. M. Finkelshtein, Pis'ma Zh. Eksp. Teor. Fiz. **46**, 407 (1987) [JETP Lett. **46**, 513 (1987)].

[34]S. Sachdev, Phys. Rev. B **39**, 5297 (1989).